ENHANCED GROWTH WITHOUT ACCELERATED PUBERTY IN FISH: A ROLE FOR THE MELANOCORTIN SYSTEM

Sandra Navarro [1], Raúl Guillot [2], Diego Crespo [3], Rüdiger W Schulz [4], Wei Ge [5], Josep Rotllant [6], José Miguel Cerdá-Reverter [2*&] and Ana Rocha [7,8*&]

[1] Centro de Investigación en Recursos Naturales y Sustentabilidad (CIRENYS), Universidad Bernardo O'Higgins, Avenida Viel 1497, Santiago de Chile

[2] Control of Food Intake Group, Department of Fish Physiolgy and Biotechnology, Instituto de Acuicultura de Torre de la Sal (IATS-CSIC), Castellón, Spain, 12595

[3] Research Group Reproduction and Developmental Biology, Institute of Marine Research, Bergen, Norway

[4] Reproductive Biology Group, Division Developmental Biology, Department Biology, Science Faculty, Utrecht University, Utrecht, The Netherlands

[5] Centre of Reproduction, Development and Aging (CRDA), Faculty of Health Sciences, University of Macau, Taipa, Macau, China

[6] Aquatic Biotechnology-ACUABIOTEC Group, Instituto de Investigaciones Marinas, Consejo Superior de Investigaciones Científicas (CSIC), Vigo, Spain

[7] Centro Interdisciplinar de Investigação Marinha e Ambiental (CIIMAR), Terminal de Cruzeiros do Porto de Leixões, 4450-208 Matosinhos, Portugal

[8] MARE – Centro de Ciências do Mar e do Ambiente, ESTM, Politécnico de Leiria, Av. Porto de Pesca, 2520-630 Peniche, Portugal

[&] Co-senior authors

[*] Correspondence: jm.cerda.reverter@csic.es; Tel.: +34-964 31 95 00 (J.M. C-R.)

anasanrocha@gmail.com; Tel.: +351-22 340 18 00 (A.R.);

ABSTRACT

In two swordtail species of the genus *Xiphophorus*, onset of puberty in males and females, fecundity in females, and adult size in males are modulated by sequence polymorphism and gene copy-number variation at the *P locus* affecting the type 4 melanocortin hormone receptor (Mc4r). The involvement of Mc4r in regulating the onset of puberty outside the genus *Xiphophorus* remains unclear. In this study we used a transgenic line overexpressing *asip1* (*asip1*-Tg), an endogenous antagonist of both type 1 melanocortin hormone receptor (Mc1r) and Mc4r, to investigate the relevance of the melanocortin system on the onset of puberty and adult reproductive performance in zebrafish (*Danio rerio*). Comparison of growth, puberty and reproductive performance between wild-type (WT) and *asip1*-Tg zebrafish revealed that a decreased activity of the melanocortin system did not change the timing of puberty but significantly delayed early growth of transgenic animals. Hatching time was postponed in *asip1*-Tg fish and they were significantly smaller than their WT siblings at 75 dpf, despite showing enhanced linear growth after having completed puberty. *asip1*-Tg females produced 1.38 times more eggs but spawned less frequently, and their eggs had showed a 0.89-fold smaller diameter but a 1.04-fold increase in larvae body length at hatching. Therefore, we demonstrate that *asip-tg* zebrafish do not reach puberty earlier than WT counterparts as it could be expected considering the enhanced length and weight growth during early adulthood. This is so because the effects of transgene on growth are noticeable from an umbral length when puberty has already been reached. Data show that the inhibition of melanocortin system via *asip* overexpression is an excellent strategy to promote growth, in absence of obesity, by enhancing food efficiency but without accelerating puberty timing. Data are crucial to provide a stepwise ahead in the characterization of the phenotype induced by the decreased activity of the melanocortin system in fish thus providing an excellent strategy for future aquaculture especially because U.S. Food and Drug Association has recently approved transgenic fish trading.

KEYWORDS: puberty; agouti-signalling protein; transgenesis; growth; sexual maturation

1. INTRODUCTION

The process through which an individual reaches sexual maturity and acquires reproductive capability is called puberty. Following gonadal sex differentiation and an immature, juvenile stage, genetic and environmental factors activate the brain-pituitary-gonadal axis, which promotes adult reproductive functions (Okuzaw, 2002; Chen and Ge, 2013). Some fish, such as swordtail species of the genus *Xiphophorus*, display a pronounced phenotypic diversity regarding puberty onset from early- (60-90 days) to late-maturing (200-300 days) polymorphs (Kallman and Schreibman 1973). This polymorphism is also associated with adult body size and reproductive behaviour in male *Xiphophorus*. Because males cease to grow reaching puberty, adult male body size is correlated with the time of sexual maturation, such that early-maturing fish are smaller than late-maturing fish (McKenzie et al., 1983). Differences in body length and the timing of puberty onset are associated with different reproductive strategies, which are key for the evolutionary fitness (Lampert et al., 2010; Maderspacher, 2010). Larger late-maturing males invest heavily in courtship by defending territories to be visited by gravid females and by ritualizing the pairing, whereas small fish exhibit a "sneaker behaviour". They do not court females but perform a chase behaviour and parasitically fertilize females just thrusting the gonopodium to obtain a copulation (Maderspacher, 2010; Liotta et al., 2019). Females prefer large and intermediate males suggesting sexual selection against sneaker alleles. However, smaller males evade predation better than larger males and have a larger time window for reproduction since they reach puberty earlier, so that reproductive success over the entire life cycle may be similar for small and large males (Maderspacher, 2010).

In the 70's, Kallman and Schreibman (1973) and Schreibman and Kallman (1977) demonstrated that a Mendelian locus on the sex chromosomes of the platyfish, the so-called *P locus* (Pituitary or Puberty), controls the onset of puberty in males and females, size in males and fecundity in females. The identity of *P locus* remained elusive for years although its position in the sex chromosomes is close to some other important loci as the sex-determining (*SD*) *locus* (*SD*), the *Tu locus*, responsible for the spontaneous melanoma (Volff et al., 2013), and some pigment genes serve as convenient gene markers of *P locus* (Schreibman and Kallman, 1977). Interestingly, the *P locus* contains multiple copies of

both functional (A allele) and non-functional versions (B1 and B2 alleles) of the melanocortin 4 receptor (*mc4r*) (Lampert et al., 2010). The size of males and, by extension, puberty onset correlate to the number of non-functional alleles in the Y chromosome. Thus, bigger males exhibit a higher number of non-functional alleles that delay puberty onset, presumably by diminishing the signalling of the functional alleles. On the contrary, males carrying functional alleles of *mc4r* are smaller and precocious (Lampert et al., 2010). Mc4r binds the melanocyte-stimulating hormones (Mshs) and two inverse agonists, agouti-related protein (Agrp) and agouti-signalling protein (Asip). Both Agrp and Asip inhibit the constitutive activity of Mc4r and antagonistically compete with α-Msh (Tolle et al., 2008; Sánchez et al., 2009) In mammals, *Mc4r* is expressed mainly in the brain but a wider expression profile is found in fish (Cerdá-Reverter et al., 2011). The hypothalamic expression is related intimately to the regulation of energy balance and growth (Cone, 2006). Therefore, the interruption of α-MSH signalling in *Mc4r* knockout mice induced hyperphagia, reduced energy expenditure, hyperinsulinemia, increased linear growth and maturity-onset obesity (Huszar et al., 1997). A similar metabolic syndrome is observed in transgenic mice ubiquitously overexpressing *Asip* or *Agrp* genes (Klebig et al., 1995; Ollmann et al., 1997). In zebrafish (*Danio rerio*), overexpression of *agrp1* (Song and Cone, 2003) and *asip1* (Guillot et al., 2016) also result in increased linear growth whereas morpholino-based *agrp* knockdown induces opposite effects (Zhang et al., 2012). The *sa0149 mc4r*-deficient zebrafish line also exhibited enhanced growth (Zhang et al., 2012) but recent results reported in medaka (*Oryzias latipes*) from de Carbio strain showed no effects on the linear growth of adult fish after TALEN-based *mc4r* knockout Liu et al., 2019).

The involvement of Mc4r in regulating the onset of puberty outside the genus *Xiphophorus* remains unclear. Even within this lineage, the molecular mechanism appears not to be conserved. While in *X. nigrensis* and *X. multilineatus*, puberty onset and body length are determined by *mc4r* allelic and copy number variations Lampert et al., 2010), in *X. hellerii*, a species where both large and small males also exist, only a wild-type (WT) *mc4r* allele was found (Liu et al., 2020). In *X. nigrensis*, *mc4r* expression in the brain is much higher in large than in small males. Such differential expression was also observed in *X. hellerii*. Hence, high expression of mc4r in large males could be related to early or late puberty

onset, reflecting an ancestral scenario in the genus *Xiphophorus*. In medaka, the regulatory network of Mc4r signalling does not appear to be involved in the regulation of puberty, as *mc4r* knockout fish reach sexual maturity at a similar time as WT animals (Liu et al., 2019). Our experiments demonstrated that *Asip1* work as an endogenous antagonist of both Mc1r and Mc4r (Cerdá-Reverter et al., 2005; Guillot et al., 2016). Subsequently, we generated a transgenic zebrafish strain overexpressing goldfish *asip1* and demonstrated the involvement of the melanocortin system in regulating the dorsoventral pigment pattern (Ceinos et al., 2015) and growth (Guillot et al., 2018). Here, we exploit the potential of this model to study the question if the decreased activity of the melanocortin system modulates the timing of puberty in zebrafish, thus expanding studies on the melanocortinergic regulation of puberty to a key model species for vertebrate development.

2. MATERIALS AND METHODS

2.1 Fish and housing

Wild-type (WT) and transgenic stocks come from a background of TU (Tuebingen, Nüsslein-Volhard Lab) strain. Generation of the transgenic zebrafish line [*Tg*(*Xla.Eef1a1:Cau.Asip1*]*iim4* (*asip1*-Tg), using the Tol2 transposon system, has been previously described (Ceinos et al., 2015). Adult zebrafish were maintained at 28 ± 2ºC under a 14 h/10 h light/dark cycle. Fish were fed three times a day until satiety with a combination of freshly-hatched brine shrimp (*Artemia sp*. nauplii) and sera Vipan flake food (Sera, Heinsberg, Germany). All experiments were performed in accordance with Spanish (Royal Decree 53/2013) and European (2010/63/EU) legislations for the protection of animals used for experimentation. The used protocols were approved by the IATS Ethics Committee (Register Number 09-0201) under the supervision of the Secretary of State for Research, Development and Innovation of the Spanish Government.

Animals used in this study were free of any signs of disease. Approximately 600 embryos of each genotype line, WT and *asip1*-Tg, were obtained at the onset of light from natural in-tank breeding crosses. Larvae from both genotypes were raised in 15 L aquarium in strictly identical conditions. From 5 to 12 dpf fish were fed rotifers. From 13 dpf they were

147 offered brine shrimp. At 20 dpf fish were transferred to two 45 L aquarium (n= 150
148 fish/aquarium) and dry food (sera Vipan flake) was gradually introduced to their diet.
149
150 *2.2 Gonadal development*
151 To increase the strength of our studies two independent experiments were conducted. In
152 experiment 1, larvae were sampled at 30, 32, 35, 40, 46, 54, 60, and 75 dpf. In experiment
153 2, sampling was conducted at 30, 34, 38, 42, 46, 60 and 75 dpf. At each sampling point, at
154 least 30 individuals were randomly collected from each tank and sacrificed by overdose of
155 tricaine methane sulfonate (MS222, 200-300 mg/L) by prolonged immersion. Larvae were
156 imaged by stereomicroscope (Olympus SZX16, stereo microscope, Tokyo, Japan), images
157 captured, and their standard length recorded using ImageJ version 1.52 software. Larvae
158 were then fixed by immersion in 1% glutaraldehyde, dehydrated, embedded in 2-
159 hydroxyethyl methacrylate polymer resin (Technovit 7100, Heraeus Kultzer, Germany).
160 Serial sections of 2 μm thickness were prepared and stained in toluidine-methylene blue
161 solution for histological analysis. Gonad morphology and classification of the ontogenetic
162 gonad differentiation into ovary or testis was done according to Maack and Segner (2003).
163 Gonads with proliferating germ cells that could not be identified as female or male germ
164 cells were classified as undifferentiated, gonads with both germ cell types in transition from
165 a bi-potential 'juvenile ovary' were classified as transitioning ovary (Supplementary Fig.
166 S1). The maturation stages were categorized using a numerical staging system based on the
167 most mature germ cells present in the gonads. Identification of germ cells at different stages
168 of gametogenesis was done according to the described above (Selman et al., 1993; Leat et
169 al., 2009). Ovarian development was classified in six stages (Supplementary Fig. S2) based
170 on their size and vitellogenic state (Wang and Ge, 2004): I, primary growth (~0.1 mm); II,
171 previtellogenic (~0.25 mm); III, early vitellogenic (~0.35 mm) ; IV, mid vitellogenic
172 (~0.45 mm) ; V, late vitellogenic (~0.55 mm) and VI, full grown (~0.65 mm). Testicular
173 development was adjusted to four stages (Supplementary Fig. S3) based on Begtashi *et al*.,
174 (2004) stage 1, immature (type A spermatogonia); stage 2, early maturation (type B
175 spermatogonia); stage 3, mid maturation (spermatogonia to spermatocytes) and stage 4, late
176 maturation (spermatocytes, spermatids, and spermatozoa).
177

178 *2.3 Maturation curve*

179 According to the histology based criteria proposed by Vazzoler (1996), a scale of three
180 maturity stages was stablished as follow: A, immature; B, maturing; C, spawning. Fish in
181 stage B and C were considered to be initiating or completing puberty. In females, puberty
182 onset is characterized by some follicles entering the previtellogenic stage (appearance of
183 cortical alveoli in the oocytes), and in males by the presence of cysts containing type B
184 spermatogonia. Fish were grouped by age (dpf) and by intervals of 2.5 mm in body length.
185 The fraction of mature fish by age, length and sex was estimated through the logistic
186 equation described by O'Brien *et al*., (1993):

187 $$P = \frac{1}{1 + e^{-(a+bX)}}$$

188 where P corresponds to the proportion of maturing fish, X the length or age and a and b are
189 the equation estimated coefficients. The parameters were estimated by a lineal regression
190 analysis using Graphpad Prism version 8.3. The length (L_{50}) and age (A_{50}) at which 50% of
191 the male and female population initiate puberty was estimated as a ratio of a/b.

192

193 *2.4 Reproductive performance*

194 Five males and five females of *asip1*-Tg or WT fish were individually placed into 2-liter
195 tanks and fed three times a day until satiety with a combination of freshly-hatched brine
196 shrimp and dry food. After 1-week acclimation, one female with bulging abdomens were
197 randomly placed into individual spawning tanks with one male and left overnight.
198 Zebrafish spawn within the first few hours after sunrise (Hisaoka and Firlit, 1962) and to
199 ensure complete spawning, the assessment of egg production took place between 8 and 10
200 am. The occurrence of a spawning event and the total number of eggs spawned per female
201 were assessed during seven spawn events. A total of thirty-five spawning couples were
202 tested for each line (five pairs per event).
203 For assessing the egg fertilization, we distinguished fertilized eggs by the presence of a
204 multi-cellular blastodisc (Kimmel et l., 1995). Fertilized eggs were collected and incubated
205 at 28°C. Mortality at 24 hpf and number of embryos hatched at 48 and 72 hpf was recorded.
206 At least 50 eggs from 3 spawning events were photographed. The egg size and diameter of
207 the yolk at the gastrulation stage were measured using ImageJ version 1.52 software. In
208 addition, at least 30 larvae of age 4 dpf were photographed individually to compare the

larval standard length- at- hatch and larval yolk sac-volume between the strain fish. The yolk-sac volume was estimated using the following formula (Chembers et al., 1989):

$$V = \pi(6LH^2)^{-1}$$

where *L* represents the length (horizontal measurement; mm) and *H* the height (vertical measurement; mm) of the yolk-sac.

2.5 Statistical analysis

Statistical treatment of the data was done with both GraphPad Prism version 8.3 The Mann-Whitney and the Kolmogorov-Smirnov nonparametric tests were used to compare the linear length between WT and *asip1*-Tg lines. To compare differences in the linear length between days, for each strain performed Dunn's test of multiple comparisons following a significant Kruskal-Wallis test. The Fisher's exact test was used for comparisons of gonadal development proportions. The strength of the association between the pair of parameters linear length and gonadal development was evaluated by calculating the correlation coefficient, r, using the Spearman rank order correlation nonparametric test. Differences in rate success spawning were analyzed by Fisher's exact test. Number of eggs and fertilized eggs, mortality, number of embryos hatched, size egg, diameter of the yolk, standard length- at- hatch and yolk sac-volume were analyzed by unpaired t test with Welch's correction. For all performed tests, the significance level was set at 0.05.

3. RESULTS

3.1 Linear Growth

The effect of overexpression of *asip1* might have on the growth of juvenile and adult zebrafish was determined by measuring standard length in both *asip1*-Tg and WT fish from 30 to 75 dpf (days post-fertilization). Two independent experiments were conducted. In experiment 1, WT zebrafish grew from 8.9 mm to 22.1 mm while *asip1*-Tg fish grew from 10.5 mm to 20.9 mm (Fig. 1A). Over the course of experiment 2, the length of WT zebrafish increased from 6.12 mm to 22.48 mm while in *asip1*-Tg it ranged from 6.5 mm to

22.4 mm (Fig. 1B). In general, for both WT and *asip1*-Tg fish, we found no significant differences in the body length during the sampling period. Exceptions include length increase in WT fish from 40 to 46 dpf and from 60 to 75 dpf in experiment 1 (Fig. 1A) and 38-42 dpf in experiment 2 (Fig. 1B). Length increase of *asip1*-Tg fish was significantly different within 35-40 dpf in experiment 1 and 46-60 dpf in experiment 2. The distribution of the standard length was significantly different among fish lines. At 30 dpf, in both experiment 1 and 2, standard length of WT was significantly lower than in *asip1*-Tg fish. However, from 42 dpf in experiment 2, 46 dpf in experiment 1, the standard length of WT was in general significantly higher than that of transgenic fish (Fig. 1). Body length data were in addition classified according to sex. For both WT and *asip1*-Tg female fish, we found no significant differences in the growth during the sampling period. Exceptions include growth increase in WT fish within 38-42 dpf in experiment 2. Regarding male fish, growth of WT was found to be significantly different but only after they attained the adult stage (Fig. 3). No differences were found in male *asip1*-Tg fish (Fig. 3). At 30 dpf (experiment 1) and 38 dpf (experiment 2), length of female WT was significantly lower than that of *asip1*-Tg (Fig. 2B). Nevertheless, at 42 dpf in experiment 2 and 46 dpf in experiment 1, this trait was reversed with WT female having a higher standard length than *asip1*-Tg females. Standard length of WT males was significantly higher than that of *asip1*-Tg males from 46 dpf until 75 dpf in experiment 2. The same trend was seen in experiment 1, although differences were statistically significant only at 75 dpf.

3.2 Gonadal differentiation

To investigate if a decreased activity of the melanocortin system induced by an overexpression of *asip1* might have a role on sexual differentiation, we monitored by histology the gonad development of *asip1*-Tg zebrafish between 30 and 75 dpf and compared these results with those found in WT fish. In experiment 1 (Fig. 4A), gonads from 226 WT fish and 237 *asip1*-Tg fish were analyzed. A female biased sex ratio was observed, with 56.6% of WT and 55.7% of *asip1*-Tg fish being identified as females. At 30 dpf (Fig. 4A2), the fraction of undifferentiated gonads was significantly higher in *asip1*-Tg than in WT fish ($p = 0.0122$), and 96.5% of WT gonads were identified as females ($p = 0.0122$) (Fig. 4A1). In both fish lines, signs of overt sexual differentiation (transitioning

phase of testis development) began at 32 dpf. However, the number of transitioning gonads was significantly higher in WT fish at 32 dpf ($p = 0.0475$) and 46 dpf ($p = 0.0237$). Male sex was revealed in gonads of 35 dpf fish. In experiment 2 (Fig. 4B), 292 gonads from WT fish were analysed and as in experiment 1, a female skewed sex ratio was observed with female representing 53.8% of the population cohort. From a total of 316 *asip1*-Tg fish, 44% were female and 51.3% male. At 30 dpf, there was no difference in the fraction of undifferentiated gonads. However, the percentage of ovaries (Fig. 4B1) was significantly higher in WT than in *asip1*-Tg fish ($p = 0.0095$) and the same was registered at 38 dpf ($p = 0.0099$). Gonads in the transitioning phase of testis development could be observed from 30 dpf onwards. The fraction of animals in the transitional phase was significantly higher in the WT line at 34 dpf ($p = 0.0136$) and 42 dpf ($p = 0.0048$). In the transgenic *asip1*-Tg line (Fig. 4B2) histological examination revealed a male fate of the gonad at 30 dpf. This sex proportion rate was significantly overrepresented at 34 ($p = 0.0007$), 38 ($p = 0.0002$) and 42 dpf ($p = 0.0010$).

3.3 Gonadal maturation

In the zebrafish, the transition from primary growth (stage I) to previtellogenesis (stage II) in the ovary is considered the sign of puberty onset in females (Ge, 2005). From 30 to 34 (experiment 1) / 35 (experiment 2) dpf, oocytes of all females, regardless of the line and trial, were at the primary growth stage (Fig. 5A, 5B). In both experiments 1 and 2, towards the end of the sampling period, the percentage of ovarian follicles in primary growth stage was higher in *asip1*-Tg females than in WT females. In experiment 1, ovarian previtellogenic follicles that are characterized by the presence of cortical alveoli oocytes were first seen at 40 dpf in the leading wave of developing oocytes. Even thought they were found initially in a similar proportion in both WT and *asip1*-Tg lines, at 46 dpf they were found in a higher percentage in WT than in *asip1*-Tg females (Fig. 5A1: 64.3%, $p = 0.0236$). In experiment 2, stage II ovaries could be recognized at 34 dpf but only in WT female (12%) and at a level not significantly different from *asip1*-Tg fish (Fig. 5B1). After the vitellogenesis stages III-V, when oocytes grow fast due to the accumulation of yolk in the cytoplasm, follicles in the ovaries of both WT and *asip1*-Tg fish entered the maturation stage (VI). In experiment 2, at 75 dpf there was a higher proportion (36.4%) of WT females

in stage VI, although this value was not significantly different from *asip1*-Tg female (5.6%). Despite puberty completion (first egg laying) was not followed in this study, the *asip1*-Tg line can be propagated in a standard propagation scheme.

In experiment 2, gonad histology analysis revealed the presence of immature testis already at 30 dpf in transgenic *asip1*-Tg fish (Fig. 6B2). In contrast, WT fish sampled at this age were still undergoing sexual differentiation (Fig. 6B1). In both experiments 1 and 2, at day 35 or 34, a higher proportion of males in stage 1 was recorded in the *asip1*-Tg line, reaching statistical significance in experiment 1 (Fig. 6). In *asip1*-Tg fish, the fraction of stage 1 testis steadily decreased until 46 dpf (when it could not be any longer recognized), when in WT at stage 1 testis, would still account for a 30.4%. The most advanced stage of testicular maturation, stage 4, could be histologically identified in *asip1*-Tg fish already at 34 dpf (20%, experiment 2) but only at 46 dpf (experiment 1: 42%, $p = 0.0239$) its proportion is significantly higher than in WT males (Fig. 6A2).

3.4 Interaction between growth and gonad development

The interaction between standard length and gonad development is illustrated in Fig. 7 and 8. In experiment 1 and 2, a strong positive association was found between these variables, irrespective of sex and genotype.

3.5 Length and age at maturity

The body length of the analyzed females varies similarly in both genotypes (experiment 1: WT = 14.9 and 22 mm; *asip1*-Tg = 14.8 y 20.9 mm and experiment 2: WT = 8.8 and 21.6 mm; *asip1*-Tg = 10.9 and 22.4 mm). The logistic function applied on female gonad maturation data shows that the body length of 15 mm in experiment 1 and 12.5 mm in experiment 2 seemed to be a threshold for reaching maturity (Fig. 9). In both experiments and for both WT and *asip1*-Tg fish, once body exceeds these lengths, and until a size of 20 mm, cortical alveoli appear and the oocytes started to accumulate in the oocytes, as a sign of transition from primary-growth to previtellogenic stages. In 22.5 mm fish, all females had reached maturity stage with full-grown follicles present in the ovary. In experiment 1, the maturity ogive estimated that the length at 50% of maturity (L_{50}) in WT and *asip1*-Tg lines was 18 mm and 17.4 mm, respectively (Fig. 9A). In experiment 2, L_{50} was estimated

as 16.2 mm for WT females and 16.7 mm for *asip1*-Tg females (Fig. 9B). As observed in females, the body length data varied similarly in both genotypes (experiment 1: WT = 11.7 and 21.3 mm; *asip1*-Tg = 13.5 and 18.9 mm and experiment 2: WT = 9.9 and 22.5 mm; *asip1*-Tg= 9.9 and 21.7 mm). The logistic function for data in experiment 1, shows that males start to mature at a smaller length than females. Between 20 and 22.5 mm, the percentage of mature males reaches 89 and 100%, respectively (Fig. 10A). On the other hand, data collected from *asip1*-Tg males, indicates that 74 and 100% of the mature male, are between 17.5 and 20 mm body length. In experiment 2, mature males from both genotypes could be observed as early as 10 mm of body length (Fig. 10B). A successive increase in the proportion of testis presenting the hallmarks of maturation was then observed. 44% of *asip1*-Tg males reached maturity with a body length of 12.5 mm while 41% of the WT males were mature with a body length of 15 mm. All males of 22.5 mm were classified as mature. In experiment 1, the maturity ogive estimated that the L_{50} for males of WT and *asip1*-Tg genotypes was 17.3 mm and 16.6 mm, respectively (Fig. 10A). In experiment 2, L_{50} was estimated as 16.5 mm for WT males and 14.4 mm for *asip1*-Tg males (Fig. 10B).

In experiment 1, the age of the sampled mature female ranged from 40 to 75 dpf. Sampling in experiment 2 allowed to identify females of the WT genotype maturing at a younger age than *asip1*-Tg females (34 and 38 dpf, respectively). The logistic function indicates that below 46 dpf (experiment 1, Fig. 11A) and 42 dpf (experiment 2, Fig. 11B), the proportion of mature females decreases and from 60 dpf onwards, more than half of the females were mature (experiment 1: WT = 79%; *asip1*-Tg = 56% and experiment 2: WT = 73%; *asip1*-Tg = 53%). At 75 dpf, 100 % of the females were mature. The maturity ogives from experiment 1 and 2 estimated that the age at 50% maturity (A_{50}) for females of the WT line was 53-54 dpf and for the *asip1*-Tg genotype was 58-59 dpf (Fig. 11A).

Regarding the males, the age of WT mature fish was similar in both experiment 1 and 2, ranging from 34 to 75 dpf. On the contrary, *asip1*-Tg males sampled during experiment 1 were found to be mature from 40 to 75 dpf, while in experiment 2, mature fish could already be identified at 30 dpf. The logistic function indicates that below 40 dpf (experiment 1, Fig. 12A) and 38 dpf (experiment 2, Fig. 12B), the proportion of mature males decreases and, as seen for female fish, the majority of the males were mature from 60

dpf onwards, reaching 100% of maturity at 75 dpf. The maturity ogives from experiment 1 and 2 estimated that the A_{50} for males of the WT line was 52-53 dpf and for the *asip1*-Tg genotype, 53 dpf in experiment 1 and 49 dpf in experiment 2 (Fig. 12A, 12B).

3.6 Reproductive performance

The rate of spawning success (that is, spawning resulting in 1 or more ova) was 97.14% for WT and 77.14% for *asip1*-Tg ($p = 0.0275$; Fig. 13A). The total number of eggs per female (mean ± SEM) was significantly ($p = 0.0113$) higher for *asip1*-Tg (493.6 ± 45.24 eggs) than for the WT line (357.8 ± 23.73 eggs; Fig. 13B). The absolute number of eggs counted for all breeding pairs for *asip1*-Tg was 13327 and 12166 for WT. Similarly, the number of fertilized eggs was significantly higher ($p = 0.0028$) for *asip1*-Tg (463.4 ± 48.37 eggs) than for WT fish (287.5 ± 27.13 eggs; Fig. 13C). However, *asip1*-Tg had a significantly higher mortality (55.5 ± 3.78 %; $p = 0.0014$) at 24 hpf compared to WT fish (36.19 ± 4.3%; Fig. 13D). However, at 48 hpf, we found significant differences in the proportion of hatched embryos ($p = 0.0205$) between WT (61.93 ± 4.95%) and *asip1*-Tg (44.62 ± 5.29%, Fig. 13E). The same was observed at 72 hpf ($p = 0.0111$), with WT having a higher proportion of hatched larvae (92.27 ± 1.94%) than *asip1*-Tg (80.96 ± 3.75%; Fig. 13F).

WT eggs were significantly larger (1.294 ± 0.0038 mm; $p < 0.0001$;) than *asip1*-Tg line eggs (1.164 ± 0.0031 mm; Fig. 14A). Eggs from WT fish also had a significantly larger diameter of yolk (0.6623 ± 0.0027 mm; $p = <0.0001$) than *asip1*-Tg (0.6028 ± 0.0021; Fig. 14B). Moreover, significant differences were also observed in the yolk-sac volume, with WT eggs presenting a bigger volume (0.0667 ± 0.0026 mm^3; $p < 0.0001$) compared to *asip1*-Tg line eggs (0.0459 ± 0.0012 mm3; Fig. 14C). On the other hand, the standard body length of freshly hatched *asip1*-Tg larvae (4 dpf) was significantly larger (3.135 ± 0.0090 mm; $p < 0.0001$) than WT (3.015 ± 0.0074 mm; Fig. 14D).

4. DISCUSSION

In teleosts, a role for Mc4r in puberty onset regulation outside *Xiphophorus* has not been described yet. Recent results in medaka have shown that Mc4r does not play any role in the timing of puberty, and mechanisms observed in *Xiphophorus* may be restricted to this lineage. To study this possibility, we here took advantage of a zebrafish line that overexpresses *asip1*, an endogenous antagonist of Mc1r and Mc4r (Cerdá-Reverter et al., 2005; Guillot et al., 2016). The *asip1*-Tg zebrafish line represents an excellent model for studies exploring the relationship between melanocortin activity and the timing of puberty onset, since overexpression of *asip1* leads to a reduction of Mc4r activity (Cerdá-Reverter et al., 2005; Sánchez et al., 2009). Our results suggest that *asip1* overexpression had no effect on the timing of puberty in zebrafish but modified growth and reproductive performance.

4.1. Growth

Previous results demonstrated that *asip1* overexpression in zebrafish enhanced linear growth (Guillot et al: 2016), but, independently of age, the first differences were detected only after a critical size close to 20 mm (Godino-Gimeno et al., 2020). Our current data show consistently that both male and female *asip1*-Tg zebrafish are significantly smaller than WT siblings at 75 dpf, when *asip1*-Tg zebrafish are just below 20 mm. However, *asip1*-Tg fish exhibit longer size at hatching despite their smaller egg and egg-yolk diameter and, by extension, smaller volume. Accordingly, knockdown of *agrp1* by morpholino techniques or the chemical ablation of agrp1 neurons in zebrafish results in shorter animals when compared to their control counterparts at 8 dpf (Zhang et al., 2012; Löhr et al., 2018). Our present data confirms that the positive effects of *asip1* overexpression, and by extension of the reduced signalling of melanocortin system, on zebrafish growth requires an umbral length close to 20 mm, just when full gonadal development is reached. Therefore, *asip1*-Tg fish hatched larger but exhibited reduced growth until completing gonadal development. From then on *asip1*-Tg fish grew faster than WT siblings, length differences reaching 15% (Guillot et al., 2016; Godino-Gimento et al., 2020).

Endocrine and molecular mechanisms promoting growth under decreased melanocortin activity have been studied but are still far from being understood. In larval zebrafish, standard somatic growth requires agrp1 signalling through mc4r (Zhang et al 2012; Godino-Gimeno et al., 2020). Therefore, *agrp1* knockdown in the morpholino zebrafish model resulted in decreased growth hormone (*gh*) expression, concomitant with increased gh-releasing hormone (*ghrh*) and decreased somatostatin I and II expression (*sstI* and *sstII*) (Zhang et al., 2012). Recently, a mechanism involving the melanocortin system in the feeding-induced growth in larval zebrafish was proposed. Overfeeding causes leptin resistance and reduced pro-opiomelanocortin (*pomc*) hypothalamic levels, leading to reduced activity of sst neurons that express Mc4r and consequently elevated *gh* expression and somatic growth (Lörh et al., 2018). It is therefore possible that *agrp1* or *asip1* overexpression in zebrafish promotes somatic growth via m sst neurons.

4.2. Timing of Puberty

Gonadal development in zebrafish can be divided in three fundamental processes: sex determination, differentiation and maintenance. While it is clear the direction in which these processes occur, the timing can be strongly variable. It is now clear, that sex of zebrafish in the wild is determined by genetic factors on a polygenic basis (Bradley et al., 2011; Anderson et al., 2012; Liew et al., 2012; Liew and Orbán, 2014). However, sex ratios in domesticate lines can be greatly influenced by environmental factors such as temperature, nutrition and population density (Lawrence et al 2008; Liew et al., 2012; Ribas et al., 2107a, Ribas et al., 2017b). In experiment 1 of our study, we observed a female skewed sex ratio in both WT and *asip1*-Tg lines that was also found in the WT population in experiment 2. The increased incidence of females in WT and *asip1*-Tg lines, indicates that equal husbandry conditions were applied to both fish populations, in particularly during the sex determination period, and that these have favor a female-biased sex ratio. Sex differentiation was first seen at 32 dpf (experiment 1) and 30 dpf (experiment 2) in both fish lines but the percentage of differentiating animals was higher in the WT line than in the *asip1*-Tg line in agreement with the delayed growth of the *asip1*-Tg line.

In the zebrafish, puberty onset depends on somatic growth rather than age (Chen and Ge, 2013; Silva et al.,2017; Hu et al 2019). Accordingly, we found a strong positive association

between growth and gonadal development in both WT and *asip1*-Tg lines. The primary-growth-to previtellogenic transition in the first cohort of developing follicles is defined as indicating female puberty onset (Ge, 2005; Taranger et al., 2010). The logistic function applied on female gonad maturation data shows that the body length of 15 mm in experiment 1 and 12.5 mm in experiment 2 seemed to be a threshold for reaching maturity in both WT and *asip1*-Tg lines. These body lengths differ from the previously reported for both female *Albino* (Chen and Ge, 2012; Chen and Ge, 2013) and Casper (White et al., 2008) zebrafish lines, that begin sexual maturation at a critical body length of 18 mm (Chen and Ge, 2013; Lessman and Brantley 2020). The Tubingen (TU) genetic background of our WT and transgenic lines could explain these observed differences since strong genetic components are known to affect size at puberty. L_{50} (length at which 50% of individuals were mature) is usually used as an index to compare maturation patterns between different groups of fish. Using our logistic model, we calculated an overall L_{50} of 17 mm (mean value of experiments 1 and 2) for both the WT and *asip1*-Tg lines. Although body length at puberty is not altered in female *asip1*-Tg, estimates of A_{50} (age at which 50% of individuals were mature) differed between genotypes with WT fish maturing younger than transgenic fish. However, the difference is only 5 days. As expected, males start to mature at a smaller length than females but at a similar time. The logistic function applied on male gonad maturation data shows that the body length of 12.5 mm in experiment 1 and 10 mm in experiment 2 seemed to be a threshold for reaching maturity in both WT and *asip1*-Tg lines. Once again, these values differ from the ones reported for males of the *Casper* zebrafish line, that begin sexual maturation at a critical body length of 17 mm (Lessman and Brantley 2020). Nevertheless, these differences should be assigned to the genetic background of the TU line. Based on our maturity ogives, the size of male *asip1*-Tg fish at maturity is slightly smaller than that of WT but the differences are minimal (0.7 mm in experiment 1 and 1.4 mm in experiment 2). Estimates of A_{50} differed between genotypes with *asip1*-Tg fish maturing 4 days younger than WT males but only in experiment 2. Overall, the data of the present study indicates that the melanocortin system is not a critical puberty signal in zebrafish as overexpression of *asip1* had no phenotypical effect on puberty timing. Our results, together with previous studies performed in medaka *mc4r* knockouts (Liu et al., 2019) and *X. hellerii*, species carrying only Mc4r functional alleles

(Liu et al., 2020), suggest that the regulation of the timing of puberty onset by Mc4r signaling in species of the genus *Xiphophorus* may be an evolutionary adaptation only fully conserved in this lineage.

4.3. Reproductive performance

Studies on MC4R-controlled pathways that regulate reproductive performance have primarily focused mice (Sandrock et al., 2009) and chicken (Aggag and El-Sabrout, 2018). Only a few studies have brought particular attention to this aspect in teleost fish. In *Xiphophorus*, *P locus* also controls female fecundity. The female genotype P^1P^1 matures earlier and produces more eggs than late maturing P^5P^5 females. Despite their larger size, P^5P^5 females consistently spawn fewer eggs than females of any other genotype (kallman and Borokoski, 1978). Different from *Xiphophorus*, we showed that *asip1*-Tg females produce more eggs than WT females but spawn less frequently. The number of fertilized eggs in *asip1*-Tg females is also higher but the hatching rate at 48 and 72h is lower. Increases in the fecundity of *asip1*-Tg females is associated with a decrease of oocyte diameter. Female oviparous vertebrates have to overcome an egg size/number commitment, thus if egg size increases, egg number decrease and vice versa (Forbes et al., 2010). The reduced size of eggs is also in agreement with a reduction in egg yolk diameter and volume. Good quality eggs often display low levels of mortality at fertilization, eying, hatch and first-feeding (Bromage et al., 1992). While there is no agreement as to what levels of mortality constitute a good quality egg, *asip1*-Tg embryonic mortality at 24h was higher than that of WT thus suggesting *asip1*-Tg eggs to have lower quality.

Yolk is the main component of freshly fertilized fish eggs and is associated to nutrients stored for embryonic development (Kawler, 2008). Eggs produced by WT fish had a larger yolk diameter than *asip1*-Tg eggs implying greater energy resource for the developing embryos. However, the standard length of hatched *asip1*-Tg larvae was significantly higher than that of WT larvae. It has been reported that larval body size results not only from growth rate of embryos and yolk-sac volume but also from efficiency of yolk energy utilization by larvae for growth and yolk energy content (Kawler, 2008). Differences in yolk energy content depend, in turn, on the size and caloric value of yolk (Kawler, 2008). Because the yolk-sac volume did differ significantly between both lines, the increased

514 standard length at hatching of *asip1*-Tg zebrafish may suggest improved use of yolk energy
515 by this line, promoting higher growth rates. We also observed that the hatching time of
516 *asip1*-Tg larvae was delayed compared to WT larvae. Delayed hatching time has also been
517 observed in mc4r knockout medaka. However, the authors concluded that contrary to our
518 results in *asip1*-Tg zebrafish, this delay is due to a decrease in the growth rate, rather than
519 an increase in the body length (Liu et al., 2020). Thickening of the outer layer of the
520 chorion makes it difficult for the embryo to break free and has been proposed to be
521 responsible for hatching delays (Uusi-Heikkilä et al., 2010). Unfortunately, we did not
522 measure chorion thickness in *asip1*-Tg embryos. In general, our findings suggest that
523 *asip1*-Tg fish have a lower reproductive performance compared to WT fishes, which is
524 reflected in lower egg quality and yolk diameter, delayed hatching time and larval growth.
525 However, further studies are needed to investigate the mechanisms behind the observed
526 differences in larval growth rate as well as yolk content between WT and *asip1*-Tg fish.
527 In summary, the regulation of the timing of the onset of puberty by the reproductive axis is
528 modulated by the growth axis. Our data further suggests an interaction of both melanocortin
529 and reproductive systems that modulates the effects of reduced melanocortin signalling on
530 somatic growth. A role of sex steroids in the modulation of these effects can be anticipated
531 but more studies are required to corroborate this hypothesis.
532
533 **5. CONCLUSION**
534 In conclusion, we demonstrate that the decreased activity of the melanocortin system
535 induced by *asip* overexpression does not accelerate the puberty timing but significantly
536 delays early growth of transgenic animals. Once *asip-tg* animals have outperformed an
537 umbral length size, close to 2cm, the transgene rapidly promotes linear growth in absence
538 of obesity by increasing both food efficiency (Godino-Gimeno et al., 2020) and food intake
539 levels (Guillot et al., 2016). Therefore, transgenic animals will become longer and heavier
540 than the WT counterparts, but no obese, during early adulthood. These animals will be
541 easily distinguished after potential escapes, since *asip* overexpression disrupts also
542 dorsoventral pigment pattern. However, consumer perception will be not affected since
543 transgene will not affect flank pigmentation (Ceinos et al., 2015). Therefore, faster growing
544 will not result into accelerate puberty that involves a major problem in farmed fish, such as

in salmonids, sea basses, flatfishes, cod fishes, tilapias, sea breams and perches. Puberty adversely affects growth, feed utilisation, health, flesh quality and welfare (Taranger et al., 2010). Reproductive performance is also affected by *asip* overexpression since *asip-tg* zebrafish spawn more eggs but less frequently and their eggs show smaller diameter *per contra* an increase in larvae body length at hatching is observed. Altogether, results provide sound data to corroborate that the decreased activity of the melanocortin system will be a crucial point in the future fish aquaculture particularly when U.S. Food and Drug Association has recently approved transgenic fish trading. Therefore, research in transgenic technology of marine species would be potentiated in order to cope next future challenges in animal production

ACKNOWLEDGMENTS

We are very grateful to José Monfort and Lucinda Rodríguez for their assistance in the histological processing of gonad samples and Joaquim Salvador for his help with animal husbandry.

FUNDING INFORMATION

This research was funded by Spanish State Agency of Research (AEI), grant number AGL2016-74857-C3-3-R and PID2019-103969RB-C33 to JMCR and AGL2017-89648P to JR, Science and Technology Foundation (FCT, Portugal), grant number PTDC/CVT-CVT/3205/2020 to AR and National Agency for Research and Development (ANID), Scholarship Program, DOCTORADO BECAS CHILE fellowship 2013–72140242 to SN.

REFERENCES

Aggag, S., El-Sabrout, K., 2018. Polymorphism of the melanocortin receptor gene and its association with egg production traits in Lohmann Brown chickens. Genetika 50, 317-323.

Anderson, J.L., Mari, A.R., Braasch, I., Amores, A., Hohenlohe, P., Batzel, P., Paul Hohenlohe, P., Batzel, P., Postlethwait, J.H., 2012. Multiple sex-associated regions and a putative sex chromosome in zebrafish revealed by RAD mapping and population genomics. PLoS ONE 7, e40701.

Begtashi, I., Rodríguez, L., Moles, G., Zanuy, S., Carrillo, M., 2004. Long-term exposure to continuous light inhibits precocity in juvenile male European sea bass (*Dicentrarchus labrax*, L.). I. Morphological aspects. Aquaculture 241, 539-559.

Bradley, K.M., Breyer, J.P., Melville, D.B., Broman, K.W., Knapik, E.W., Smith, J.R., 2011. An SNP-based linkage map for zebrafish reveals sex determination loci. G3 (Bethesda) 1, 3-9.

Bromage, N., Jones, J., Randall, C., Thrush, M., Davies, B., Springate, J., Duston, J., Barker, G., 1992. Broodstock management, fecundity, egg quality and the timing of egg production in the rainbow trout (*Oncorhynchus mykiss*). Aquaculture 100, 141-166.

Ceinos, R.M., Guillot, R., Kelsh, R.N., Cerdá-Reverter, J.M., Rotllant, J., 2015. Pigment patterns in adult fish result from superimposition of two largely independent pigmentation mechanisms. Pigment Cell Melanoma Res. 28, 196-209.

Cerdá-Reverter, J.M., Agulleiro, M.J., Guillot, R., Sánchez, E., Ceinos, R., Rotllant, J., 2011. Fish melanocortin system. Eur. J. Pharmacol. 660, 53-60.

Cerdá-Reverter, J.M., Haitina, T., Schiöth, H.B., Peter, R.E. 2005. Gene structure of the goldfish agouti-signaling protein: a putative role in the dorsal-ventral pigment pattern of fish. Endocrinology 146, 1597-1610.

Chambers, R., Leggett, W., Brown, J., 1989. Egg size, female effects, and the correlation between early life history traits of capelin *Mallotus villosus*: an appraisal at the individual level. Fish Bull. U.S. 87, 515-523.

Chen, W., Ge, W., 2013. Gonad differentiation and puberty onset in the zebrafish: Evidence for the dependence of puberty onset on body growth but not age in females. Mol. Reprod. Dev. 80, 384-392.

598 Chen, W., Ge, W., 2012. Ontogenic expression profiles of gonadotropins (fshb and lhb) and
599 growth hormone (gh) during sexual differentiation and puberty onset in female zebrafish.
600 Biol. Reprod. 86, 73.
601 Cone, R.D., 2006. Studies on the physiological functions of the melanocortin system. Endocr.
602 Rev. 2006 27, 736-749.
603 Forbes, E.L., Preston, C.D., Lokman, P.M., 2010. Zebrafish (*Danio rerio*) and the egg size
604 versus egg number trade off: effects of ration size on fecundity are not mediated by
605 orthologues of the Fec gene. Reprod. Fertil. Dev. 22, 1015-1021.
606 Ge, W., 2005. Intrafollicular paracrine communication in the zebrafish ovary: the state of the
607 art of an emerging model for the study of vertebrate folliculogenesis. Mol. Cell.
608 Endocrinol. 237, 1-10.
609 Godino-Gimeno, A., Sánchez, E., Guillot, R., Rocha, A., Angotzi, A.R., Leal, E., Rotllant, J.,
610 Cerdá-Reverter, J.M., 2020. Growth performance after agouti-signaling protein 1 (Asip1)
611 overexpression in transgenic zebrafish. Zebrafish 17, 373-381.
612 Guillot, R., Cortés, R., Navarro, S., Mischitelli, M., García-Herranz, V., Sánchez, E., Cal, L.,
613 Navarro, J.C., Míguez, J.M., Afanasyev, S., Krasnov, A., Cone, R.D., Rotllant, J., Cerdá-
614 Reverter, J.M., 2016. Behind melanocortin antagonist overexpression in the zebrafish brain:
615 a behavioral and transcriptomic approach. Horm. Behav. 82, 87-100.
616 Hisaoka, K., Firlit, C., 1962. Ovarian cycle and egg production in the zebrafish, *Brachydanio*
617 *rerio*. Copeia. 4, 788-792.
618 Hu, Z., Ai, N., Chen, W., Wong, Q.W.-L., Ge, W., 2019. Loss of growth hormone gene (GH1)
619 in zebrafish arrests folliculogenesis in females and delays spermatogenesis in males.
620 Endocrinology 160, 568-586.
621 Huszar, D., Lynch, C.A., Fairchild-Huntress, V., Dunmore, J.H., Fang, Q., Berkemeier, L.R.,
622 Gu W, Kesterson, R.A., Boston, B.A., Cone, R.D., Smith, F.J., Campfield, L.A., Burn, P.,
623 Lee, F., 1997. Targeted disruption of the melanocortin-4 receptor results in obesity in mice.
624 Cell 88, 131-141.
625 Kallman, K.D., Borkoski, V., 1978. A sex-linked gene controlling the onset of sexual maturity
626 in female and male platyfish (*Xiphophorus maculatus*), fecundity in females and adult size
627 in males. Genetics 89, 79-119.

628 Kallman, K.D., Schreibman, M.P., 1973. A sex-linked gene controlling gonadotrop
629 differentiation and its significance in determining the age of sexual maturation and size of
630 the platyfish, *Xiphophorus maculatus*. Gen. Comp. Endocrinol. 21, 287-304.
631 Kamler, E., 2008. Resource allocation in yolk-feeding fish. Rev. Fish Biol. Fish. 18,143-200.
632 Kimmel, C.B., Ballard, W.W., Kimmel, S.R., Ullmann, B., Schilling, T.F., 1995. Stages of
633 embryonic development of the zebrafish. Dev. Dyn. 203, 253-310.
634 Klebig, M., Wilkinson, J., Geisler, J., Woychik, R., 1995. Ectopic expression of the agouti
635 gene in transgenic mice causes obesity, features of type II diabetes, and yellow fur. Proc.
636 Natl. Acad. Sci. USA 92, 4728-4732.
637 Lampert, K.P., Schmidt, C., Fischer, P., Volff, J.-N., Hoffmann, C., Muck, J., Lohse, M.J.,
638 Ryan, M.J., Schartl, M., 2010. Determination of onset of sexual maturation and mating
639 behavior by melanocortin receptor 4 polymorphisms. Curr. Biol. 20, 1729-1734.
640 Lawrence, C., Ebersole, J.P., Kesseli, R.V., 2008. Rapid growth and out-crossing promote
641 female development in zebrafish (*Danio rerio*). Environ. Biol. Fish. 81, 239-246.
642 Leal MC, Cardoso ER, Nóbrega RH, Batlouni SR, Bogerd J, França LR, Schulz, R.W., 2009.
643 Histological and stereological evaluation of zebrafish (*Danio rerio*) spermatogenesis with
644 an emphasis on spermatogonial generations. Biol. Reprod. 81, 177-187.
645 Lessman, C.A., Brantley, N.A., 2020. Puberty visualized: sexual maturation in the transparent
646 Casper zebrafish. Zygote 28, 322-332.
647 Liew, W.C., Bartfai, R., Lim, Z., Sreenivasan, R., Siegfried, K.R., Orban, L., 2012. Polygenic
648 sex determination system in zebrafish. PLoS ONE 7, e34397.
649 Liew, W.C., Orbán, L., 2014. Zebrafish sex: a complicated affair. Brief. Funct. Genomics 13,
650 172-187.
651 Liotta, M.N., Abbott, J.K., Rios-Cardenas, O., Morris, M.R., 2019. Tactical dimorphism: the
652 interplay between body shape and mating behaviour in the swordtail *Xiphophorus*
653 *multilineatus* (Cyprinodontiformes: Poeciliidae). Biol. J. Linn. Soc. 127, 337-350.
654 Liu, R., Du, K., Ormanns, J., Adolfi, M.C., Schartl, M., 2020. Melanocortin 4 receptor
655 signaling and puberty onset regulation in *Xiphophorus* swordtails. Gen. Comp. Endocrinol.
656 295,113521.
657 Liu, R., Kinoshita, M., Adolfi, MC., Schartl, M., 2019. Analysis of the role of the Mc4r
658 system in development, growth, and puberty of medaka. Front. Endocrinol. 10, 213.

659 Löhr H, Hess S, Pereira MM, Reinoß P, Leibold S, Schenkel C, Wunderlich, C.M.,
660 Kloppenburg, P., Brüning, J.C., Hammerschmidt, M., 2018. Diet-induced growth is
661 regulated via acquired leptin resistance and engages a pomc-somatostatin-growth hormone
662 circuit. Cell Rep. 23, 1728-1741.
663 Maack, G., Segner, H. 2003. Morphological development of the gonads in zebrafish. J. Fish
664 Biol. 62, 895-906.
665 Maderspacher, F., 2010. Reproductive strategies: how big is your love? Curr. Biol. 20, R925-
666 R928.
667 McKenzie, Jr. W.D., Crews, D., Kallman, K.D., Policansky, D., Sohn, J.J., 1983. Age, weight
668 and the genetics of sexual maturation in the platyfish, *Xiphophorus maculatus*. Copeia.
669 1983, 770-774
670 O'Brien, L., Burnett, J., Mayo, R.K., 1993. Maturation of nineteen species of finfish off the
671 northeast coast of the United States, 1985-1990. NOAA Tech. Rep. NMFS 113.
672 Okuzawa, K., 2002. Puberty in teleosts. Fish Physiol. Biochem. 26, 31-41.
673 Ollmann, M.M., Wilson, B.D., Yang, Y.-K., Kerns, J.A., Chen, Y., Gantz, I., Barsh, G.S.,
674 1997. Antagonism of central melanocortin receptors *in vitro* and *in vivo* by agouti-related
675 protein. Science 278, 135-138.
676 Ribas, L., Liew, W.C., Díaz, N., Sreenivasan, R., Orbán, L., Piferrer, F., 2017. Heat-induced
677 masculinization in domesticated zebrafish is family-specific and yields a set of different
678 gonadal transcriptomes Proc. Natl. Acad. Sci. USA 114, E941-E950.
679 Ribas, L., Valdivieso, A., Díaz, N., Piferrer, F., 2017. Appropriate rearing density in
680 domesticated zebrafish to avoid masculinization: links with the stress response. J. Exp.
681 Biol. 220:1056-1064.
682 Sánchez, E., Rubio, V.C., Thompson, D., Metz, J., Flik, G., Millhauser, G.L., Cerdá-Reveerer,
683 JM., 2009. Phosphodiesterase inhibitor-dependent inverse agonism of agouti-related protein
684 on melanocortin 4 receptor in sea bass (*Dicentrarchus labrax*). Am. J. Physiol. Regul.
685 Integr. Comp. Physiol. 296, R1293-R306.
686 Sandrock, M., Schulz, A., Merkwitz, C., Schöneberg, T., Spanel-Borowski, K., Ricken, A.,
687 2009. Reduction in corpora lutea number in obese melanocortin-4-receptor-deficient mice.
688 Reprod. Biol. Endocrinol. 7, 24.

689 Schreibman, M.P., Kallman, K.D., 1977. The genetic control of the pituitary-gonadal axis in
690 the platyfish, *Xiphophorus maculatus*. J. Exp. Zool. 200, 277-293.
691 Selman, K., Wallace, R.A., Sarka, A., Qi, X., 1993. Stages of oocyte development in the
692 zebrafish, *Brachydanio rerio*. J. Morphol. 218, 203-224.
693 Silva, A.C.G., Almeida, D.V., Nornberg, B.F., Pereira, J.R., Pires, D.M., Corcini, C.D., Varela
694 A.S. Jr., Marins L.F.., 2017. Reproductive parameters of double transgenic zebrafish
695 (*Danio rerio*) males overexpressing both the growth hormone (GH) and its receptor (GHR).
696 Transgenic Res. 26, 123-134.
697 Song, Y., Cone, R.D., 2007. Creation of a genetic model of obesity in a teleost. FASEB J. 21,
698 2042-2049.
699 Taranger, G.L., Carrillo, M., Schulz, R.W., Fontaine, P., Zanuy, S., Felip, A., Finn-Arne
700 Weltzien, F.-A., Dufour, S., Karlsen, O., Norberg, B., Andersson, E., Hansen, T., 2010.
701 Control of puberty in farmed fish. Gen. Comp. Endocrinol. 165, 483-515.
702 Tolle, V., Low, M.J., 2008. In vivo evidence for inverse agonism of Agouti-related peptide in
703 the central nervous system of proopiomelanocortin-deficient mice. Diabetes 57, 86-94.
704 Uusi-Heikkilä, S., Wolter, C., Meinelt, T., Arlinghaus, R., 2010. Size-dependent reproductive
705 success of wild zebrafish *Danio rerio* in the laboratory. J. Fish Biol. 77, 552-569.
706 Vazzoler A.E.A. de M. Biologia da reprodução de peixes teleósteos: teoria e prática. EDUEM,
707 Maringá, BR, 1996.
708 Volff, J.-N., Selz, Y., Hoffmann, C., Froschauer, A., Schultheis, C., Schmidt, C., Zhou, Q.,
709 Bernhardt, W., Hanel, R., Böhne, A., Brunet, F., Ségurens, B., Couloux, A., Bernard-
710 Samain, S., Barbe, V., Ozouf-Costaz, C., Galiana, D., Lohse, M.J., Schartl M., 2013. Gene
711 amplification and functional diversification of melanocortin 4 receptor at an extremely
712 polymorphic locus controlling sexual maturation in the platyfish. Genetics 195, 1337-1352.
713 Wang, Y., Ge, W., 2004. Developmental profiles of activin βA, βB, and follistatin expression
714 in the zebrafish ovary: evidence for their differential roles during sexual maturation and
715 ovulatory cycle. Biol. Reprod. 71, 2056-2064.
716 White, R.M., Sessa, A., Burke, C., Bowman, T., LeBlanc, J., Ceol, C., Bourque, C., Dovey,
717 M., Goessling, W., Erter Burns, C., Zon, L.I., 2008. Transparent adult zebrafish as a tool
718 for *in vivo* transplantation analysis. Cell Stem Cell 2, 183-189.

719 Zhang, C., Forlano, P.M., Cone, R.D., 2012. AgRP and POMC neurons are hypophysiotropic
720 and coordinately regulate multiple endocrine axes in a larval teleost. Cell Metab. 15, 256-
721 264.
722

FIGURE LEGENDS

Figure 1. Standard length of WT and *asip1*-Tg fish in (**A**) experiment 1 and (**B**) experiment 2. Data are represented as mean ± SD. Numbers inside the bars indicate sample size (n). Statistical significance is indicated as asterisks (*). For all statistics: *p < 0.05, **p < 0.01, ***p < 0.001, ****p <0.0001.

Figure 2. Standard length of WT and *asip1*-Tg female fish in (**A**) experiment 1 and (**B**) experiment 2. Data are represented as mean ± SD. Statistical significance is indicated as asterisks (*).

Figure 3. Standard length of WT and *asip1*-Tg male fish in (**A**) experiment 1 and (**B**) experiment 2. Data are represented as mean ± SD. Statistical significance is indicated as asterisks (*).

Figure 4. Gonadal differentiation of WT and *asip1*-Tg fish in (**A**) experiment 1 (**A1**: WT; **A2**: *asip1*-Tg) and (**B**) experiment 2 (**B1**: WT; **B2**: *asip1*-Tg). Data are represented as a percentage of the total number of fish analyzed for each genotype. Statistical significance after Fisher's exact test is indicated as asterisks (*).

Figure 5. Ovary development of WT and *asip1*-Tg fish in (**A**) experiment 1 (**A1**: WT; **A2**: *asip1*-Tg) and (**B**) experiment 2 (**B1**: WT; **B2**: *asip1*-Tg). Data are represented as a percentage of the total number of fish analyzed for each genotype. Statistical significance after Fisher's exact test is indicated as asterisks (*).

Figure 6. Testis development of WT and *asip1*-Tg fish in (**A**) experiment 1 (**A1**: WT; **A2**: *asip1*-Tg) and (**B**) experiment 2 (**B1**: WT; **B2**: *asip1*-Tg). Data are represented as a percentage of the total number of fish analyzed for each genotype. Statistical significance after Fisher's exact test is indicated as asterisks (*).

Figure 7. Correlation analysis to evaluate the strength of relationship between ovary development and standard length of WT and *asip1*-Tg fish in (**A**) experiment 1 (**A1**: WT; **A2**: *asip1*-Tg) and (**B**) experiment 2 (**B1**: WT; **B2**: *asip1*-Tg). The degree of association between variables was measured with the Spearman's rank correlation test with a statistical significance of p< 0.05.

Figure 8. Correlation analysis to evaluate the strength of relationship between testis development and standard length of WT and *asip1*-Tg fish in (**a**) experiment 1 (**A1**: WT;

754 **A2**: *asip1*-Tg) and (**B**) experiment 2 (**B1**: WT; **B2**: *asip1*-Tg). The degree of association
755 between variables was measured with the Spearman's rank correlation test with a statistical
756 significance of $p< 0.05$.
757 **Figure 9.** Female first sexual maturity ogives by length based on the histological analysis
758 of ovaries of WT and *asip1*-Tg fish in (**A**) experiment 1 and (**B**) experiment 2. Black circle
759 (●) represents observed data for WT female; Dash (-) represents estimates for WT females;
760 Black square (■) represents observed data for *asip1*-Tg female; Double dash (--) represents
761 estimates for *asip1*-Tg female.
762 **Figure 10.** Male first sexual maturity ogives by length based on the histological analysis of
763 testis of WT and *asip1*-Tg fish in (**A**) experiment 1 and (**B**) experiment 2. Black circle (●)
764 represents observed data for WT male; Dash (-) represents estimates for WT males; Black
765 square (■) represents observed data for *asip1*-Tg male; Double dash (--) represents
766 estimates for *asip1*-Tg male.
767 **Figure 11.** Female first sexual maturity ogives by age based on the histological analysis of
768 ovaries of WT and *asip1*-Tg fish in (**A**) experiment 1 and (**B**) experiment 2. Black circle
769 (●) represents observed data for WT female; Dash (-) represents estimates for WT females;
770 Black square (■) represents observed data for *asip1*-Tg female; Double dash (--) represents
771 estimates for *asip1*-Tg female.
772 **Figure 12.** Male first sexual maturity ogives by age based on the histological analysis of
773 testis of WT and *asip1*-Tg fish in (**A**) experiment 1 and (**B**) experiment 2. Black circle (●)
774 represents observed data for WT male; Dash (-) represents estimates for WT males; Black
775 square (■) represents observed data for *asip1*-Tg male; Double dash (--) represents
776 estimates for *asip1*-Tg male.
777 **Figure 13.** Effect of asip1 overexpression on adult zebrafish reproductive function and
778 offspring viability. Average of spawning events (**A**), number eggs per female (**B**), number
779 fertilized eggs (**C**), egg mortality at 24 hpf (**D**), hatched at 48 hpf (**E**) and hatched at 72 hpf
780 (**F**). All data represent the mean± SEM. Statistical significance is indicated as asterisks (*),
781 $*p < 0.05$, $**p < 0.01$.
782 **Figure 14.** Morphological assessment of offspring. Average of egg size (**A**), egg yolk
783 diameter (**B**), larval yolk-sac volume (**C**) and larval standard length (Ls)-at-hatch (**D**). All

784 data are represented as the mean± SEM. Statistical significance is indicated as asterisks (*),
785 *p < 0.05, ****p <0.0001.

SUPPLEMENTAL INFORMATION

Supplementary Figure S1. Morphological gonad types of the zabrafish. (**A**) Undifferentiated gonads are characterized by the presence of germ cells (GC). (**B**) Ovaries containing densely packed oocytes at the primary growth stage (PG). (**C**) Transitioning ovaries contains a few degenerative oocytes (DO) that may develop into residual body-like structures (RB). Stromal cells (SC) represent the majority of the gonad. (**D**) Testes is occupied by different types of spermatogonia (Spg) where cyst-like arranged gonial cells (Cy). SM: Skeletal muscle; In: Intestine; Pa: Pancreas; SB: Swim bladder; Li: Liver.

Supplementary Figure S2. Zebrafish ovaries of different developmental stages. (**A**) Stage I: primary growth (PG). (**B**) Stage II: previtellogenic (PV).(**C**) Stage III: early vitellogenic (EV). (**D**) Stage IV: mid vitellogenic (MV). (**E**) Stage V: late vitellogenic (LV). (**F**) Stage VI: full grown (FG)

Supplementary Figure S3. Zebrafish testes of different developmental stages. (**A**) Stage 1: immature. (**B**) Stage 2: early maturation. (**C**) Stage 3: mid maturation. (**D**) Stage 4: late maturation. SPG Aund: type A undifferentiated spermatogonia; SPG Adiff: type A differentiated spermatogonia; SPG B: type B spermatogonia; SPC: spermatocytes; SPT: spermatids; SPZ: spermatozoa.

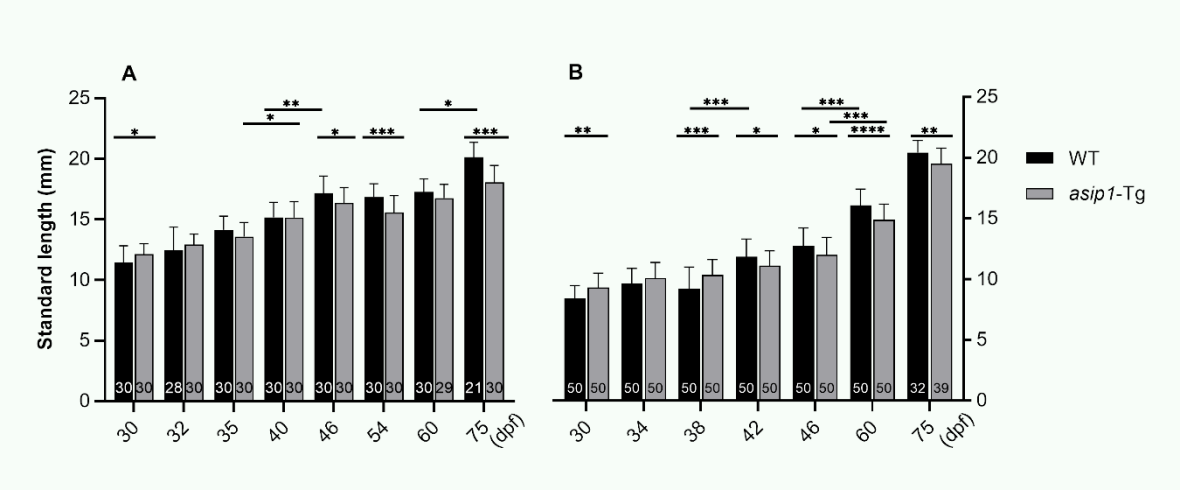

Figure 1. Standard length of WT and *asip1*-Tg fish in (**A**) experiment 1 and (**B**) experiment 2. Data are represented as mean ± SD. Numbers inside the bars indicate sample size (n). Statistical significance is indicated as asterisks (*). For all statistics: *p < 0.05, **p < 0.01, ***p < 0.001, ****p <0.0001.

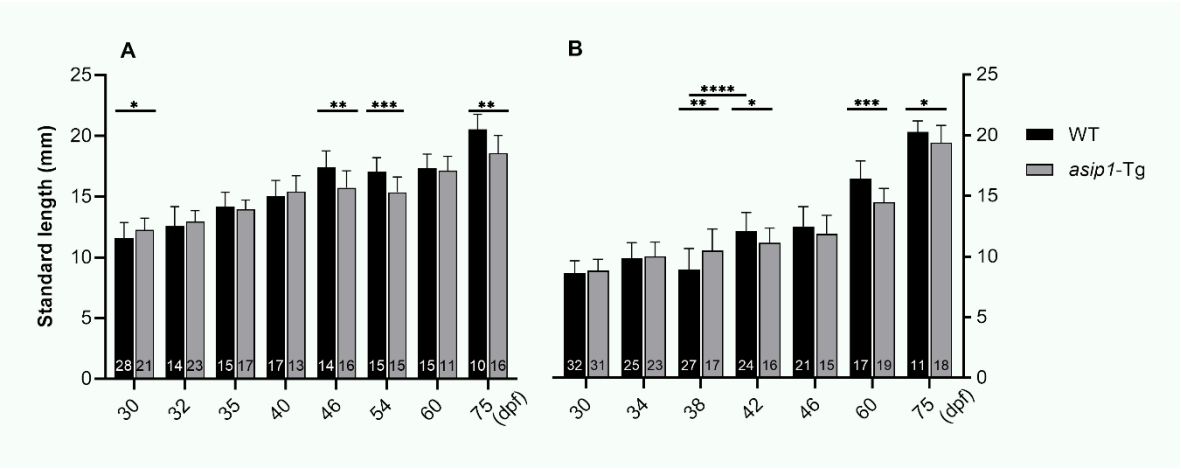

Figure 2. Standard length of WT and *asip1*-Tg female fish in (**A**) experiment 1 and (**B**) experiment 2. Data are represented as mean ± SD. Numbers inside the bars indicate sample size (n). Statistical significance is indicated as asterisks (*).

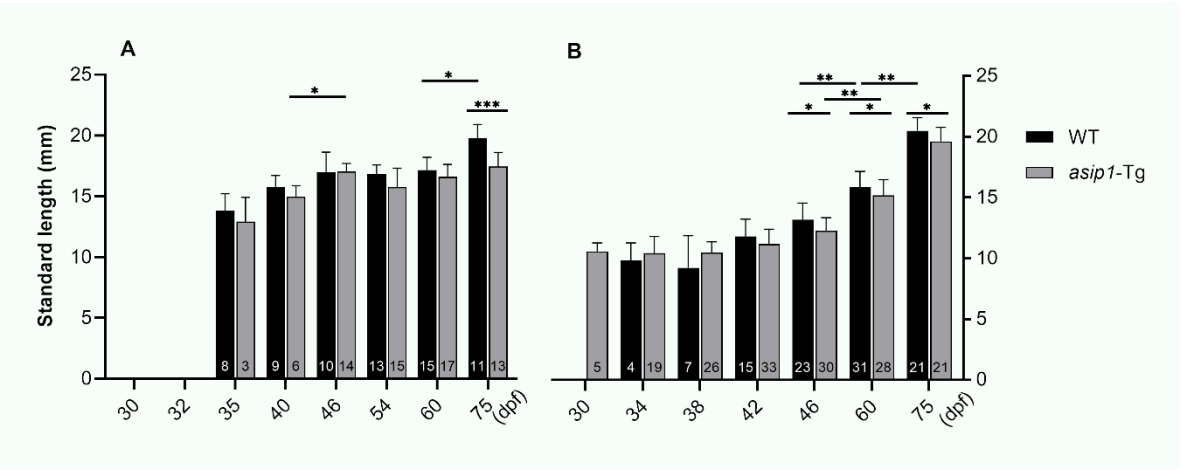

Figure 3. Standard length of WT and *asip1*-Tg male fish in (**A**) experiment 1 and (**B**) experiment 2. Data are represented as mean ± SD. Numbers inside the bars indicate sample size (n). Statistical significance is indicated as asterisks (*).

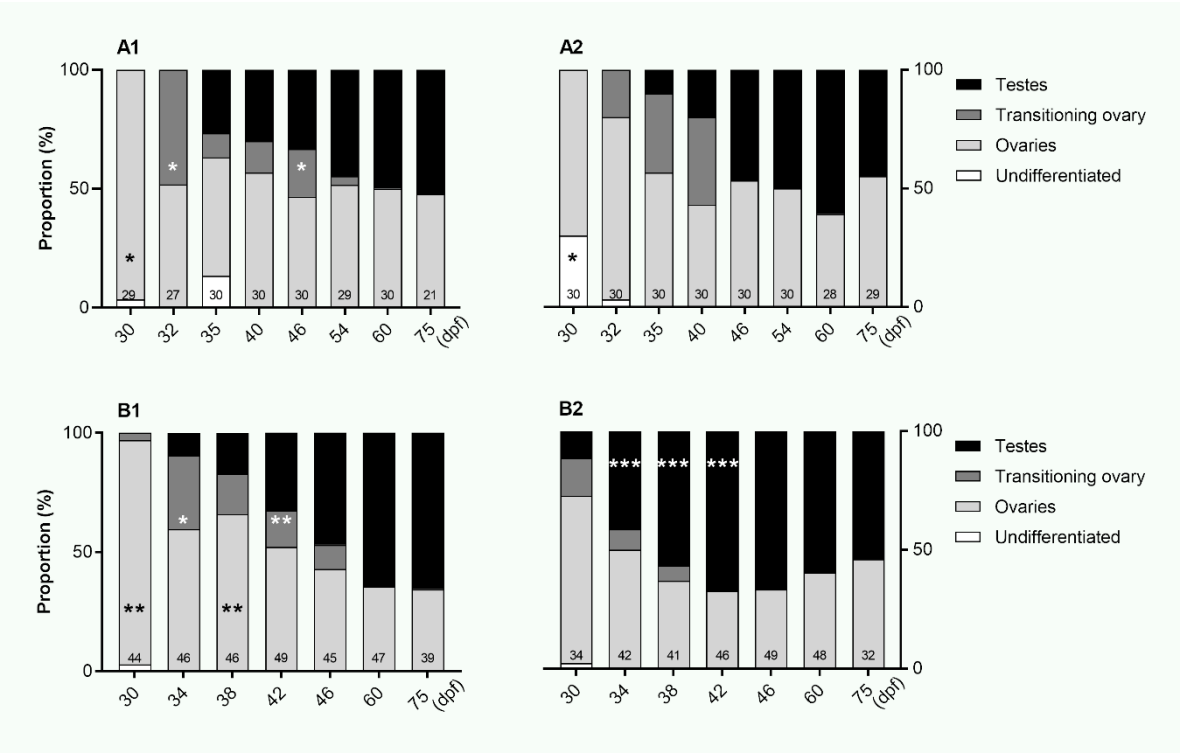

Figure 4. Gonadal differentiation of WT and *asip1*-Tg fish in (**A**) experiment 1 (**A1**: WT; **A2**: *asip1*-Tg) and (**B**) experiment 2 (**B1**: WT; **B2**: *asip1*-Tg). Data are represented as a percentage of the total number of fish analyzed for each genotype. Numbers inside the bars indicate sample size (n). Statistical significance after Fisher's exact test is indicated as asterisks (*).

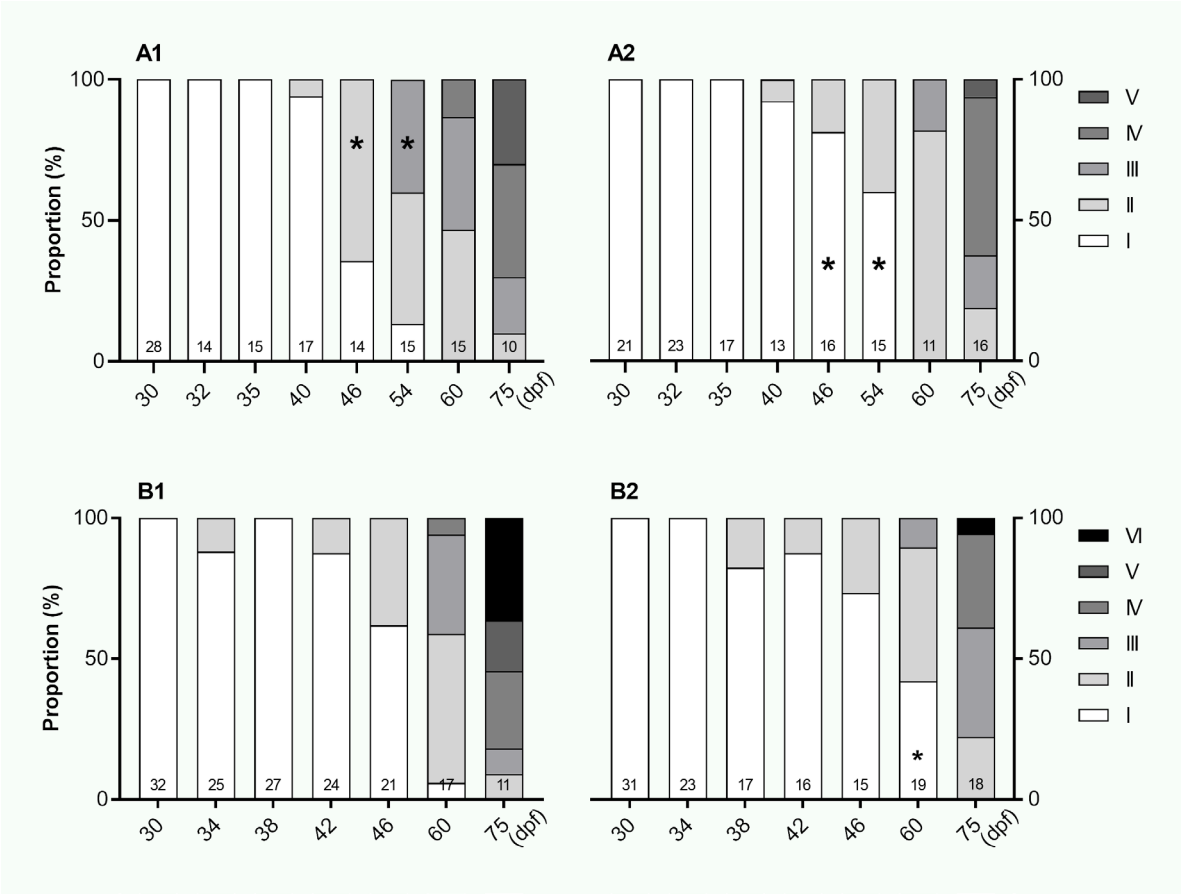

867

868 **Figure 5.** Ovary development of WT and *asip1*-Tg fish in (**A**) experiment 1 (**A1**: WT; **A2**:
869 *asip1*-Tg) and (**B**) experiment 2 (**B1**: WT; **B2**: *asip1*-Tg). Data are represented as a
870 percentage of the total number of fish analyzed for each genotype. Numbers inside the bars
871 indicate sample size (n). Statistical significance after Fisher's exact test is indicated as
872 asterisks (*).

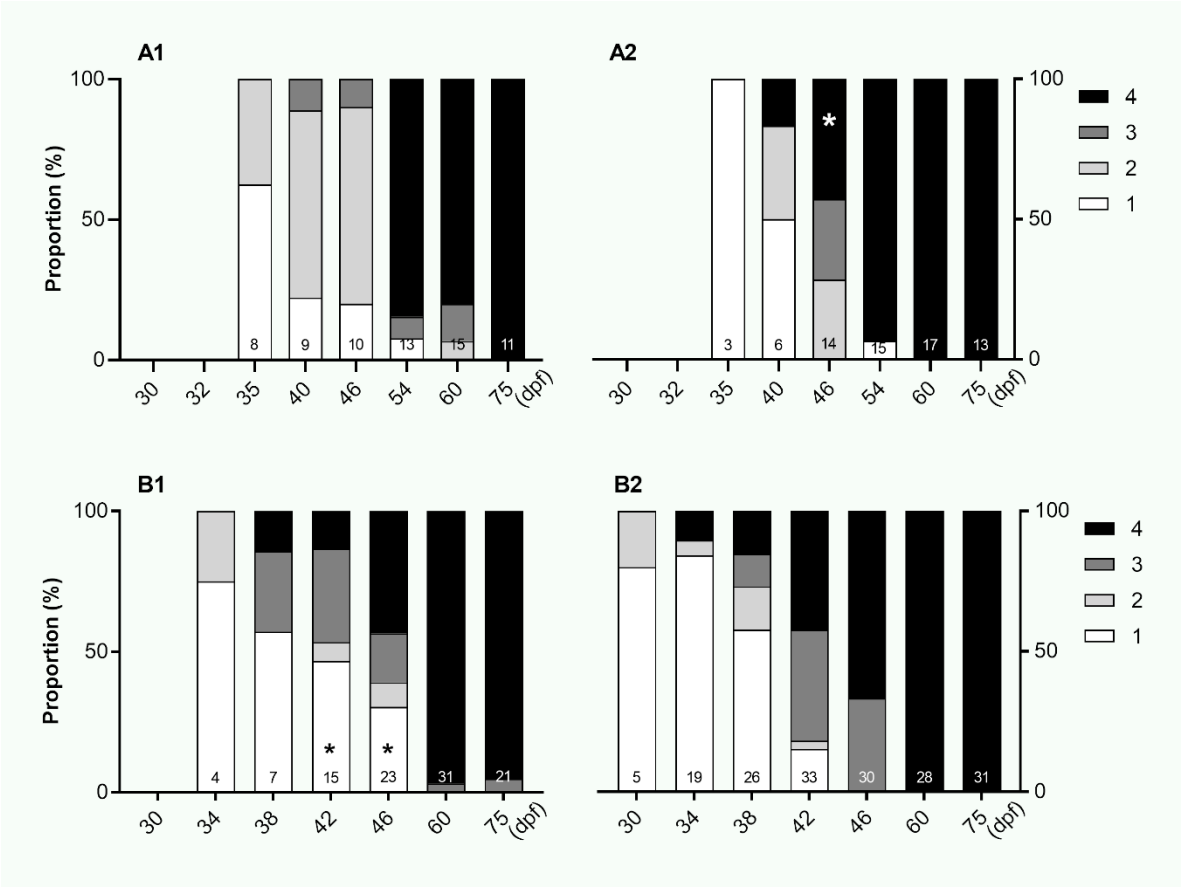

Figure 6. Testis development of WT and *asip1*-Tg fish in (**A**) experiment 1 (**A1**: WT; **A2**: *asip1*-Tg) and (**B**) experiment 2 (**B1**: WT; **B2**: *asip1*-Tg). Data are represented as a percentage of the total number of fish analyzed for each genotype. Statistical significance after Fisher's exact test is indicated as asterisks (*).

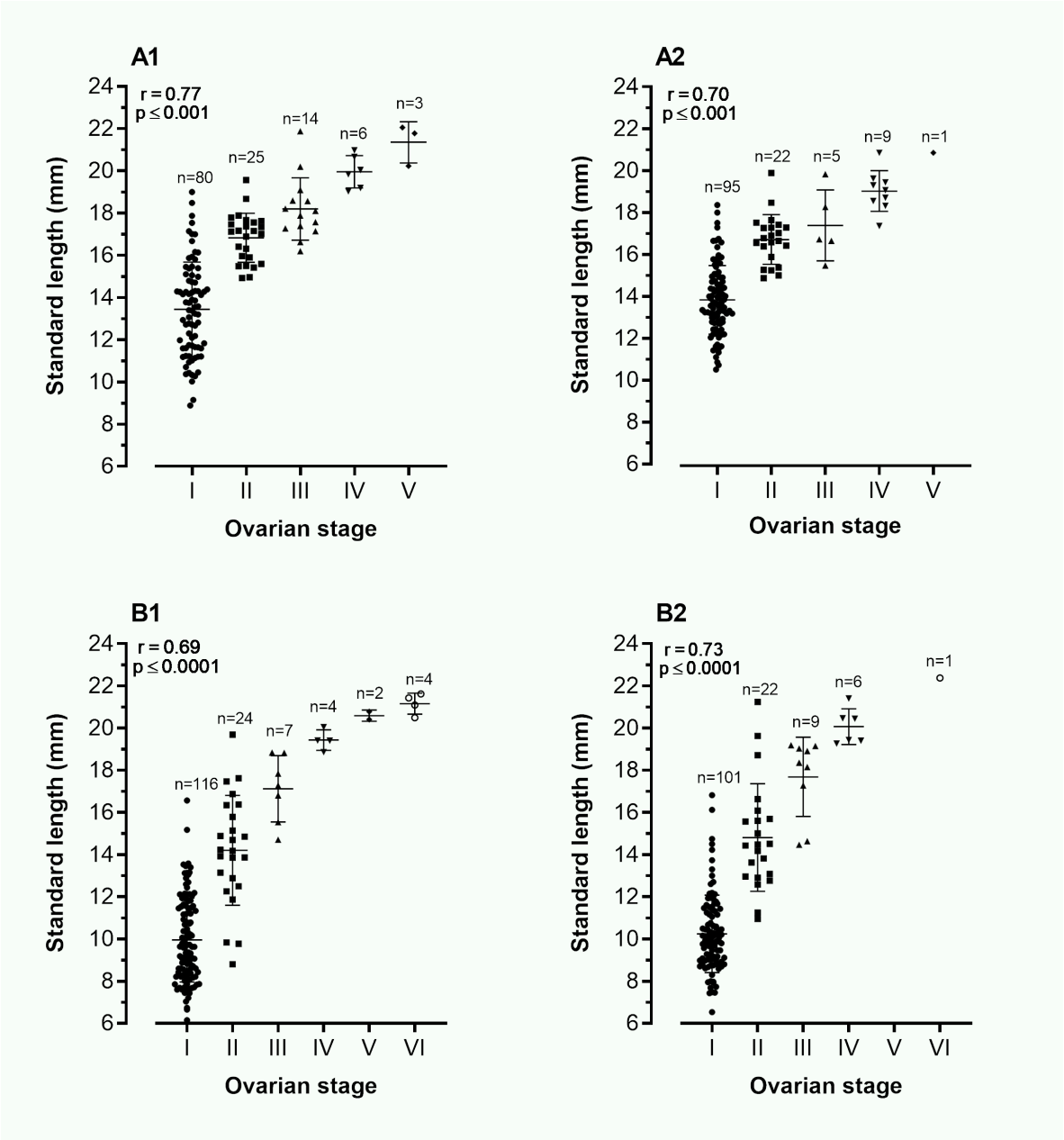

Figure 7. Correlation analysis to evaluate the strength of relationship between ovary development and standard length of WT and *asip1*-Tg fish in (**A**) experiment 1 (**A1**: WT; **A2**: *asip1*-Tg) and (**B**) experiment 2 (**B1**: WT; **B2**: *asip1*-Tg). The degree of association between variables was measured with the Spearman's rank correlation test with a statistical significance of $p < 0.05$.

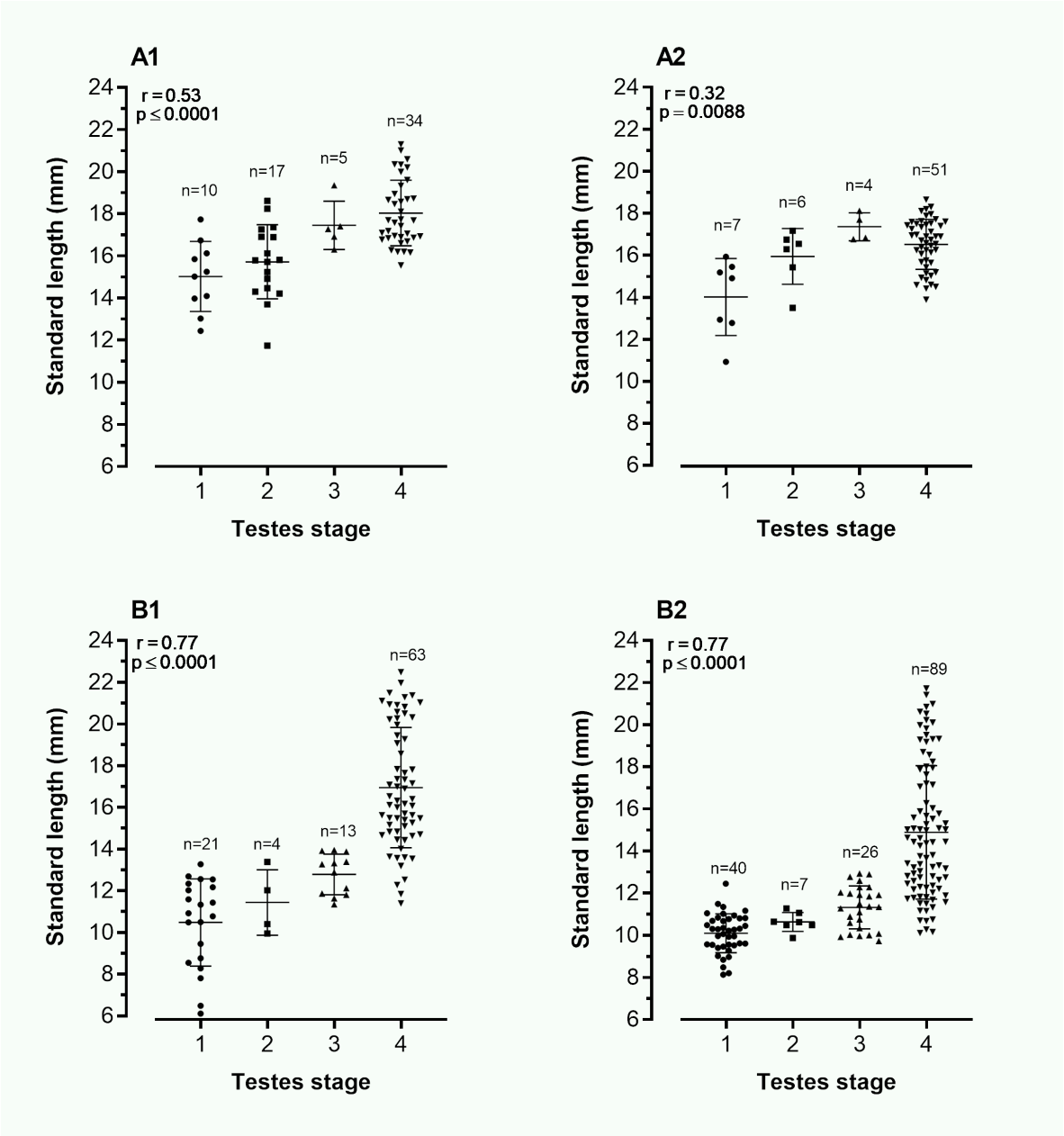

Figure 8. Correlation analysis to evaluate the strength of relationship between testis development and standard length of WT and *asip1*-Tg fish in (**a**) experiment 1 (**A1**: WT; **A2**: *asip1*-Tg) and (**B**) experiment 2 (**B1**: WT; **B2**: *asip1*-Tg). The degree of association between variables was measured with the Spearman's rank correlation test with a statistical significance of $p < 0.05$.

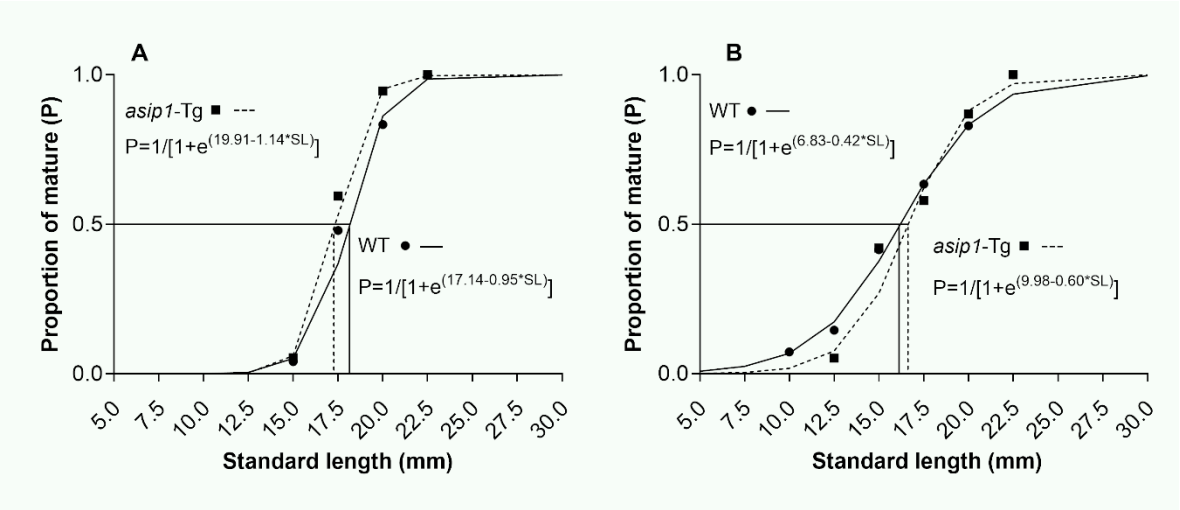

911 **Figure 9.** Female first sexual maturity ogives by length based on the histological analysis
912 of ovaries of WT and *asip1*-Tg fish in (**A**) experiment 1 and (**B**) experiment 2. Black circle
913 (●) represents observed data for WT female; Dash (-) represents estimates for WT females;
914 Black square (■) represents observed data for *asip1*-Tg female; Double dash (--) represents
915 estimates for *asip1*-Tg female.
916
917

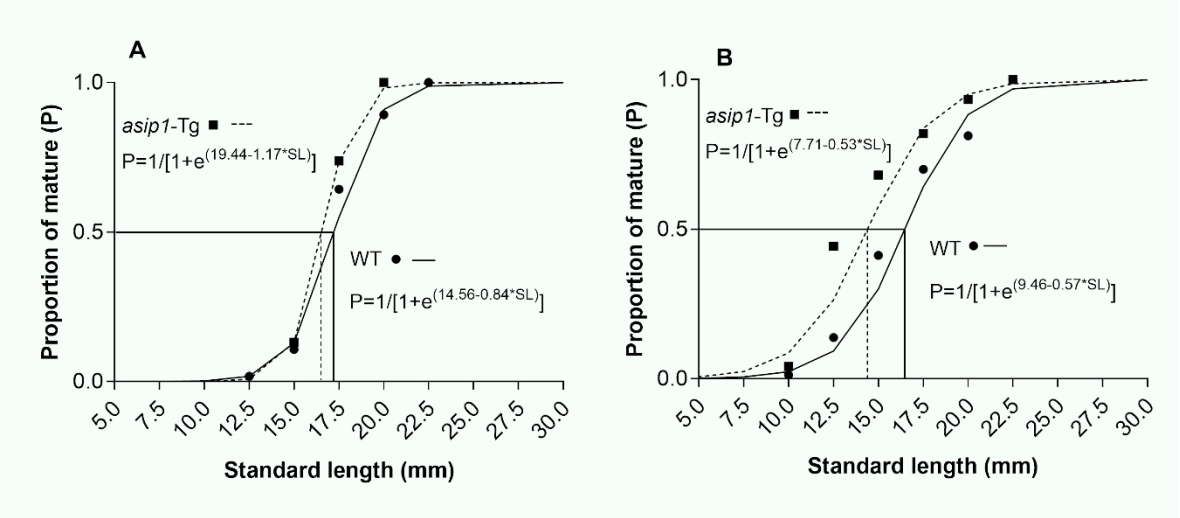

918 **Figure 10.** Male first sexual maturity ogives by length based on the histological analysis of
919 testis of WT and *asip1*-Tg fish in (**A**) experiment 1 and (**B**) experiment 2. Black circle (●)
920 represents observed data for WT male; Dash (-) represents estimates for WT males; Black
921 square (■) represents observed data for *asip1*-Tg male; Double dash (--) represents
922 estimates for *asip1*-Tg male.
923

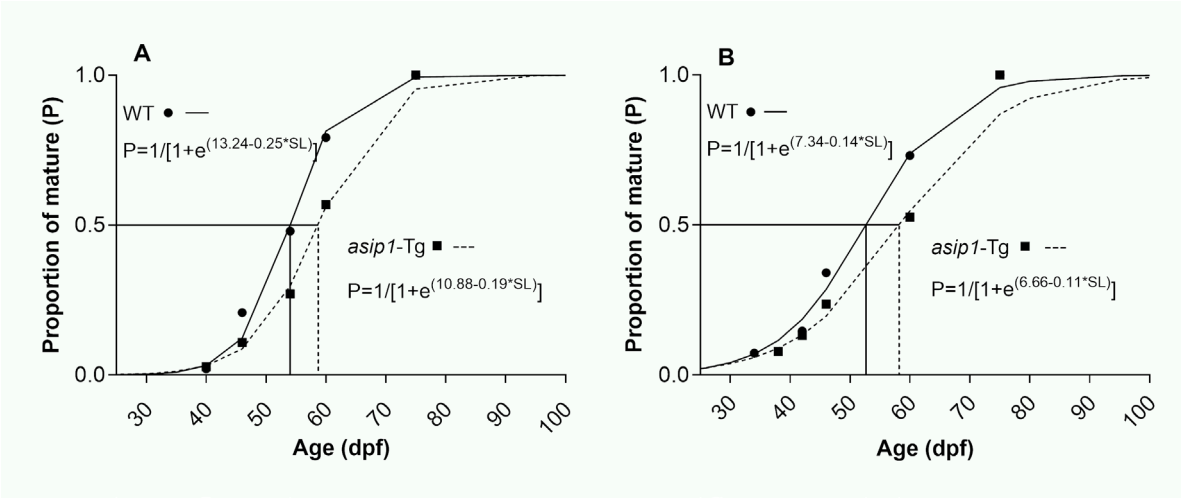

Figure 11. Female first sexual maturity ogives by age based on the histological analysis of ovaries of WT and *asip1*-Tg fish in (**A**) experiment 1 and (**B**) experiment 2. Black circle (●) represents observed data for WT female; Dash (-) represents estimates for WT females; Black square (■) represents observed data for *asip1*-Tg female; Double dash (--) represents estimates for *asip1*-Tg female.

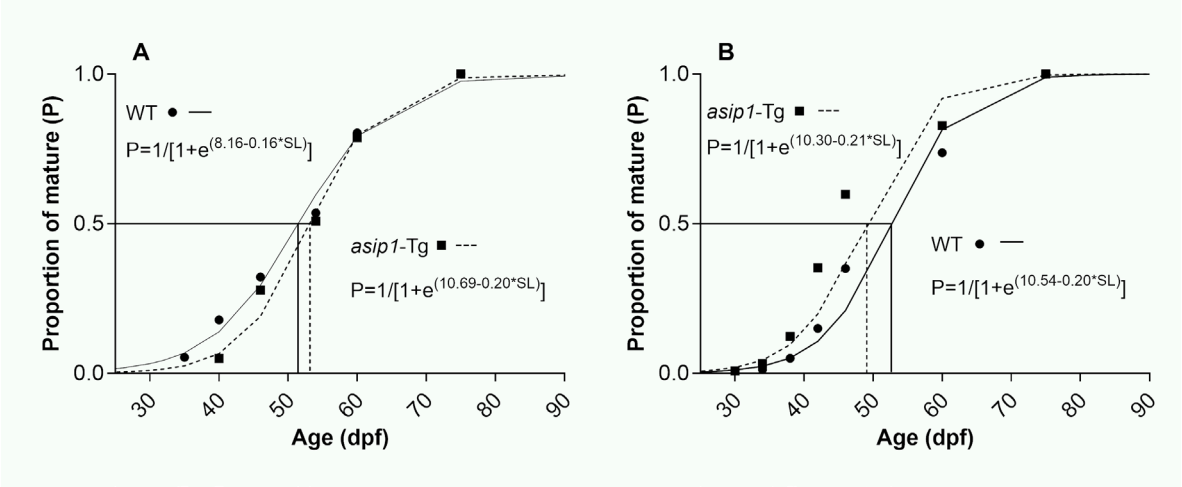

Figure 12. Male first sexual maturity ogives by age based on the histological analysis of testis of WT and *asip1*-Tg fish in (**A**) experiment 1 and (**B**) experiment 2. Black circle (●) represents observed data for WT male; Dash (-) represents estimates for WT males; Black square (■) represents observed data for *asip1*-Tg male; Double dash (--) represents estimates for *asip1*-Tg male.

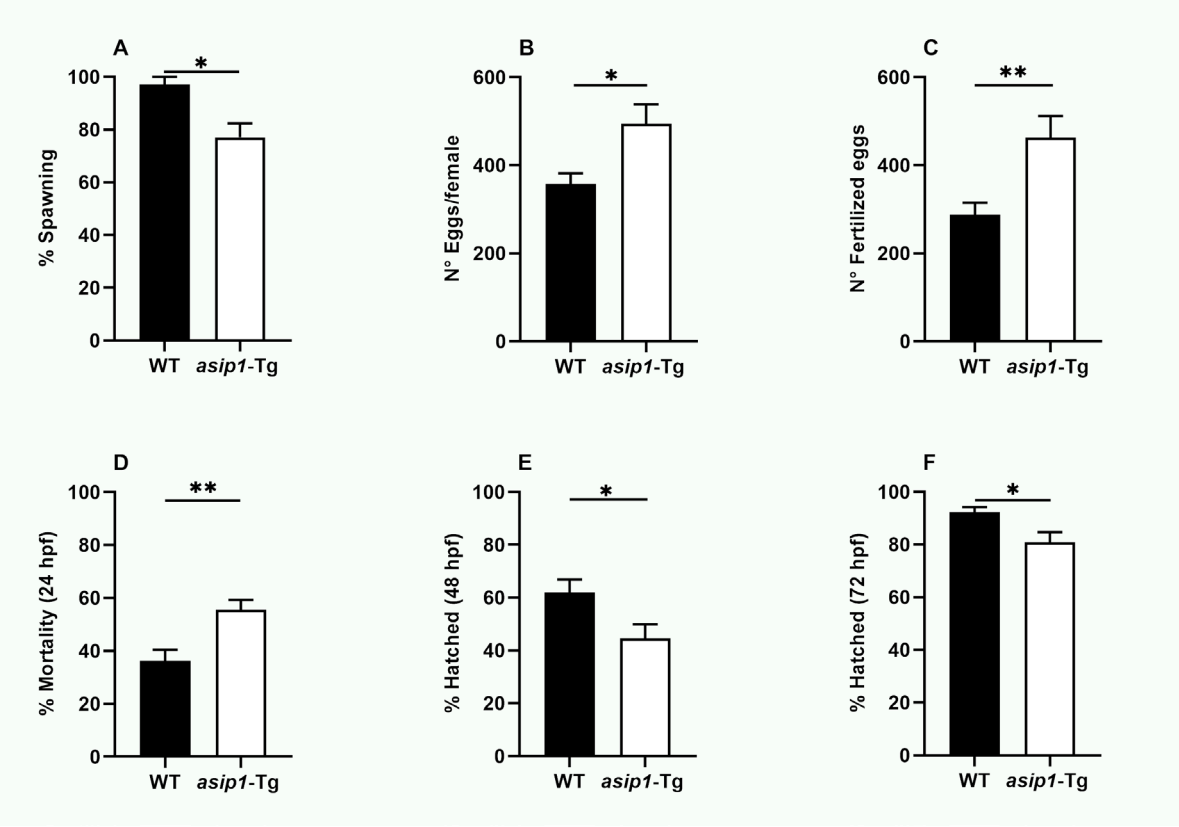

Figure 13. Effect of asip1 overexpression on adult zebrafish reproductive function and offspring viability. Average of spawning events (**A**), number eggs per female (**B**), number fertilized eggs (**C**), egg mortality at 24 hpf (**D**), hatched at 48 hpf (**E**) and hatched at 72 hpf (**F**). All data represent the mean± SEM. Statistical significance is indicated as asterisks (*), *$p < 0.05$, **$p < 0.01$.

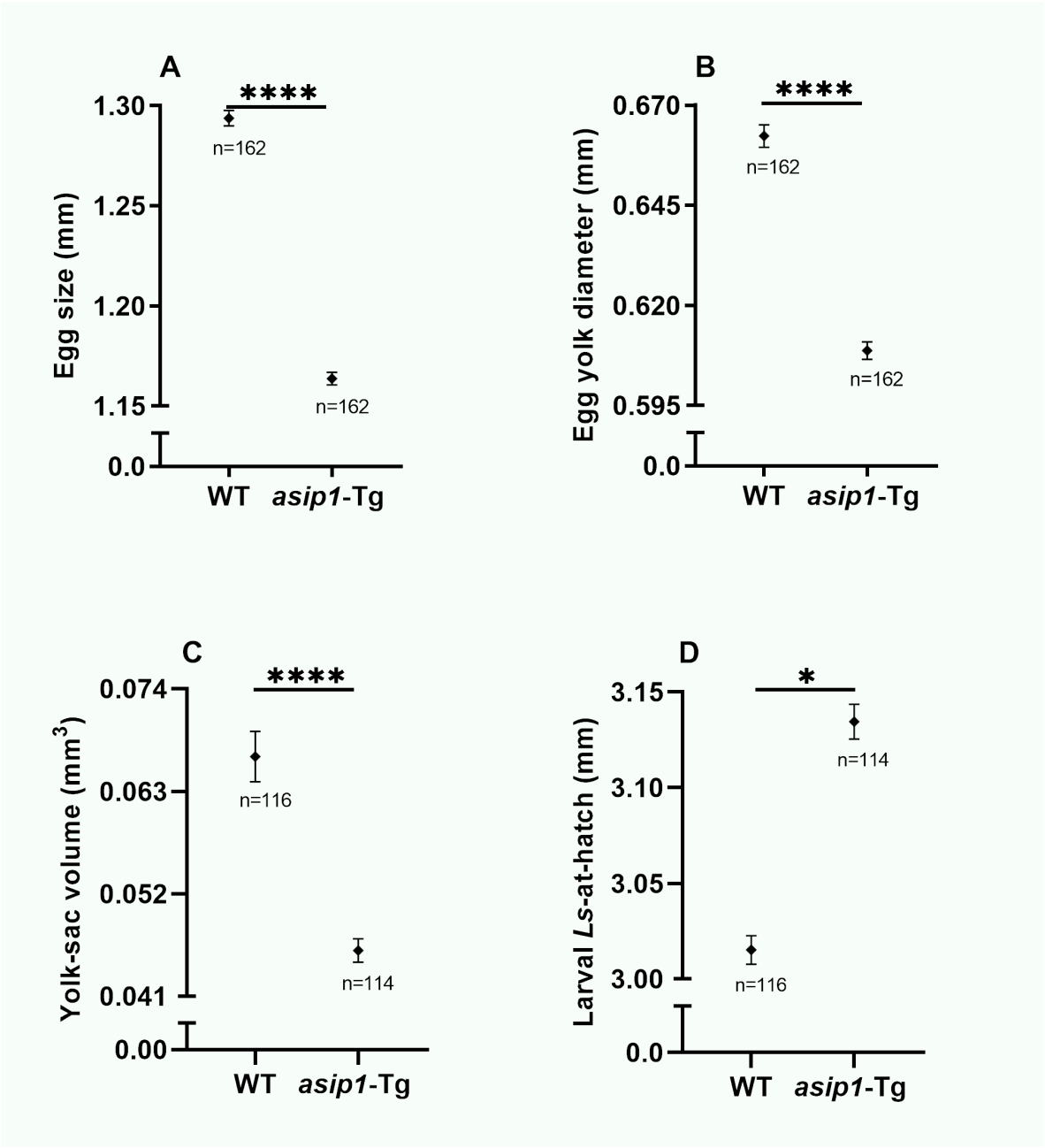

Figure 14. Morphological assessment of offspring. Average of egg size (**A**), egg yolk diameter (**B**), larval yolk-sac volume (**C**) and larval standard length (Ls)-at-hatch (**D**). All data are represented as the mean± SEM. Statistical significance is indicated as asterisks (*), *$p < 0.05$, ****$p < 0.0001$.

SUPPLEMENTARY INFORMATION

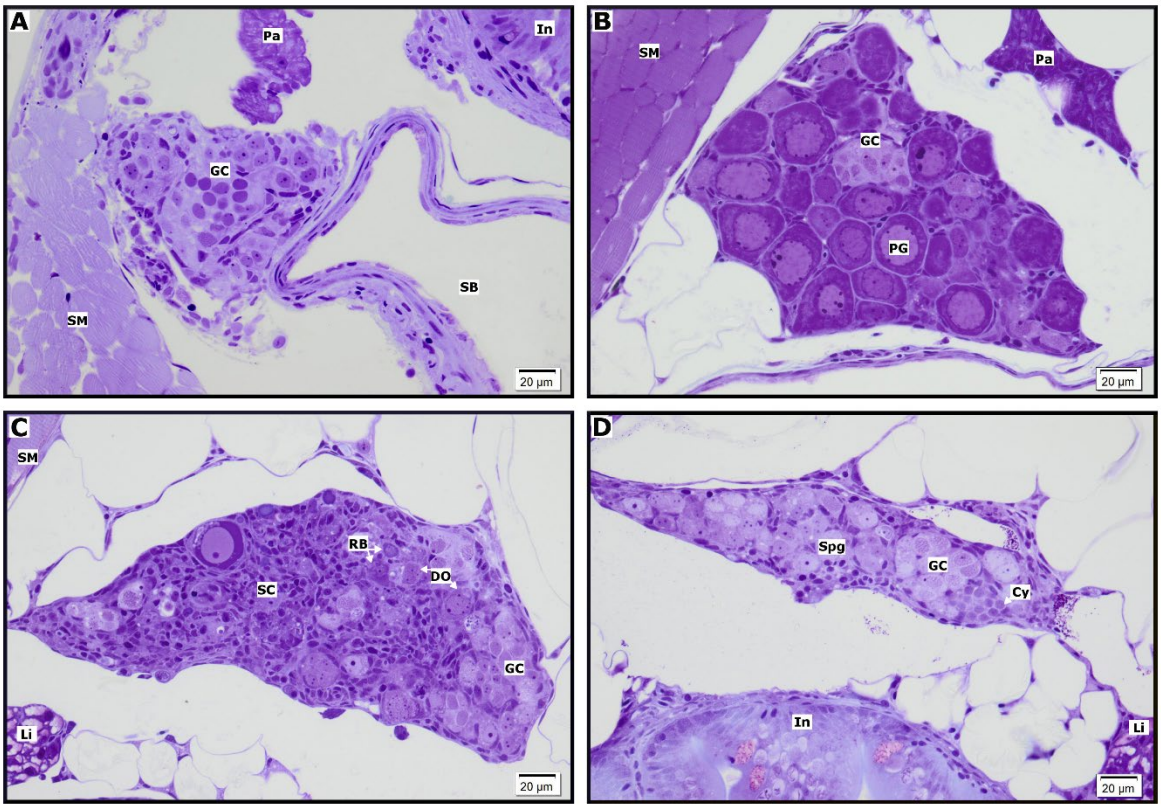

Supplementary Figure S1. Morphological gonad types of the zabrafish. (**A**) Undifferentiated gonads are characterized by the presence of germ cells (GC). (**B**) Ovaries containing densely packed oocytes at the primary growth stage (PG). (**C**) Transitioning ovaries contains a few degenerative oocytes (DO) that may develop into residual body-like structures (RB). Stromal cells (SC) represent the majority of the gonad. (**D**) Testes is occupied by different types of spermatogonia (Spg) where cyst-like arranged gonial cells (Cy). SM: Skeletal muscle; In: Intestine; Pa: Pancreas; SB: Swim bladder; Li: Liver.

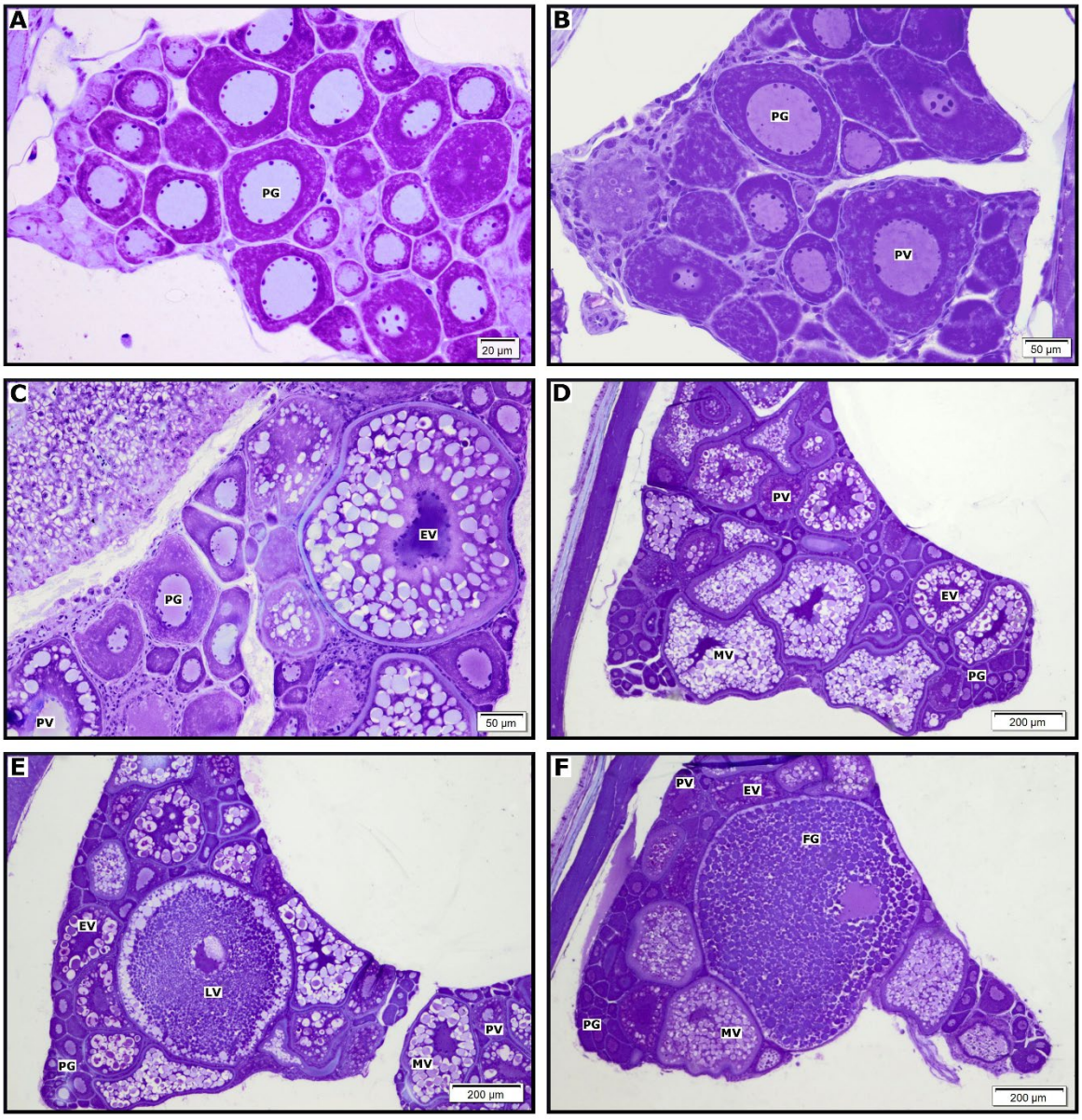

Supplementary Figure S2. Zebrafish ovaries of different developmental stages. (**A**) Stage I: primary growth (PG). (**B**) Stage II: previtellogenic (PV).(**C**) Stage III: early vitellogenic (EV). (**D**) Stage IV: mid vitellogenic (MV). (**E**) Stage V: late vitellogenic (LV). (**F**) Stage VI: full grown (FG)

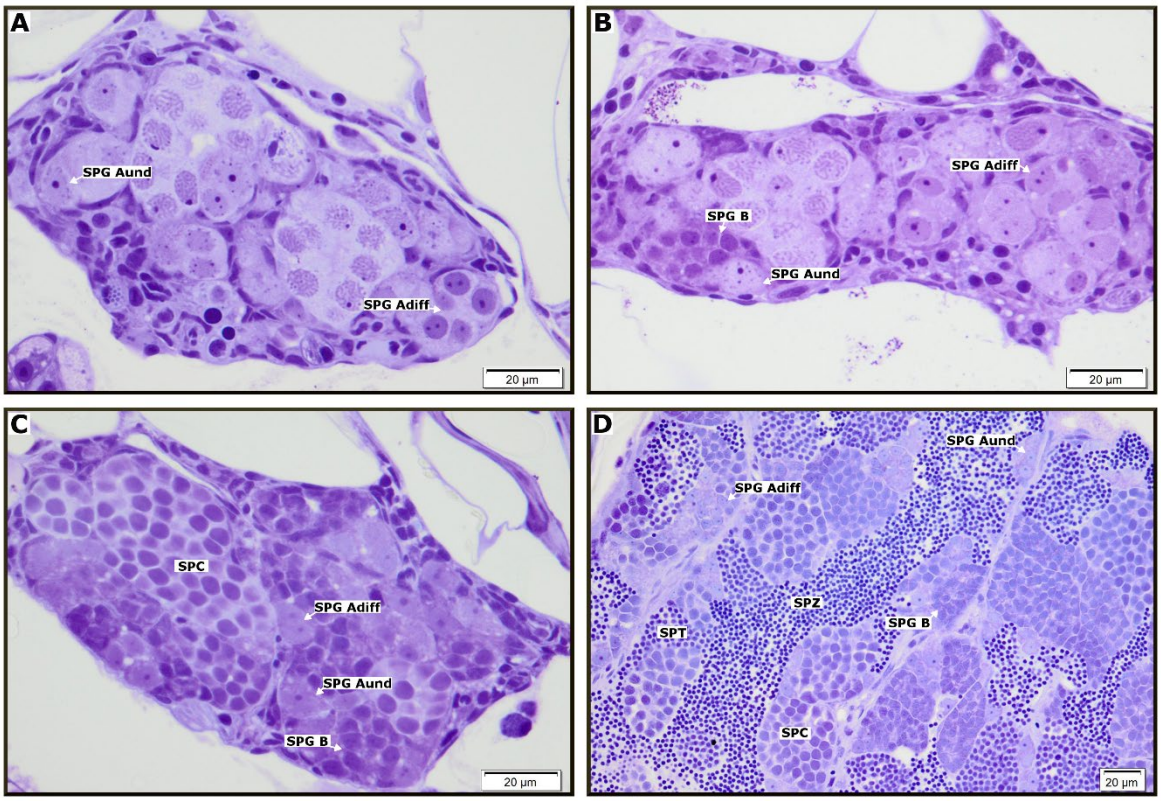

Supplementary Figure S3. Zebrafish testes of different developmental stages. (**A**) Stage 1: immature. (**B**) Stage 2: early maturation. (**C**) Stage 3: mid maturation. (**D**) Stage 4: late maturation. SPG Aund: type A undifferentiated spermatogonia; SPG Adiff: type A differentiated spermatogonia; SPG B: type B spermatogonia; SPC: spermatocytes; SPT: spermatids; SPZ: spermatozoa.